

Searching for the signatures of terrestrial planets in F-, G-type main-sequence stars [★]

J. I. González Hernández^{1,2}, E. Delgado-Mena³, S. G. Sousa³, G. Israelian^{1,2}, N. C. Santos^{3,4}, V. Zh. Adibekyan³, and S. Udry⁵

¹ Instituto de Astrofísica de Canarias (IAC), E-38205 La Laguna, Tenerife, Spain
e-mail: jonay@iac.es

² Depto. Astrofísica, Universidad de La Laguna (ULL), E-38206 La Laguna, Tenerife, Spain

³ Centro de Astrofísica, Universidade do Porto, Rua das Estrelas, 4150-762 Porto, Portugal

⁴ Departamento de Física e Astronomia, Faculdade de Ciências, Universidade do Porto, Portugal

⁵ Observatoire Astronomique de l'Université de Genève, 51 Ch. des Maillettes, -Sauverny- Ch1290, Versoix, Switzerland

Received July 24, 2012; accepted January 9, 2013

ABSTRACT

Context. Detailed chemical abundances of volatile and refractory elements have been discussed in the context of terrestrial-planet formation during in past years.

Aims. The HARPS-GTO high-precision planet-search program has provided an extensive database of stellar spectra, which we have inspected in order to select the best-quality spectra available for late type stars. We study the volatile-to-refractory abundance ratios to investigate their possible relation with the low-mass planetary formation.

Methods. We present a fully differential chemical abundance analysis using high-quality HARPS and UVES spectra of 61 late F- and early G-type main-sequence stars, where 29 are planet hosts and 32 are stars without detected planets.

Results. As for the previous sample of solar analogs, these stars slightly hotter than the Sun also provide very accurate Galactic chemical abundance trends in the metallicity range $-0.3 < [\text{Fe}/\text{H}] < 0.4$. Stars with and without planets show similar mean abundance ratios. Moreover, when removing the Galactic chemical evolution effects, these mean abundance ratios, $\Delta[\text{X}/\text{Fe}]_{\text{SUN-STARS}}$, against condensation temperature tend to exhibit less steep trends with nearly zero or slightly negative slopes. We have also analyzed a subsample of 26 metal-rich stars, 13 with and 13 without known planets, with spectra at $S/N \sim 850$, on average, in the narrow metallicity range $0.04 < [\text{Fe}/\text{H}] < 0.19$. We find the similar, although not equal, abundance pattern with negative slopes for both samples of stars with and without planets. Using stars at $S/N \geq 550$ provides equally steep abundance trends with negative slopes for stars both with and without planets. We revisit the sample of solar analogs to study the abundance patterns of these stars, in particular, 8 stars hosting super-Earth-like planets. Among these stars having very low-mass planets, only four of them reveal clear increasing abundance trends versus condensation temperature.

Conclusions. Finally, we compared these observed slopes with those predicted using a simple model that enables us to compute the mass of rocks that have formed terrestrial planets in each planetary system. We do not find any evidence supporting the conclusion that the volatile-to-refractory abundance ratio is related to the presence of rocky planets.

Key words. stars: abundances — stars: fundamental parameters — planetary systems — stars: atmospheres

1. Introduction

In the past decade, the exhaustive search for extrasolar planets has given rise to a significant collection of high-quality spectroscopic data (see e.g. Marcy et al. 2005; Udry & Santos 2007). In particular, the HARPS-GTO high-precision planet-search program (Mayor et al. 2003) has conducted in the first five years an intensive tracking of F-, G-, and K-type main-sequence stars in the solar neighborhood, resulting in the discovery of an increasing population of Neptune and super-Earth-like planets (Mayor & Udry 2008; Mayor et al. 2011). Interestingly,

the very strong correlation observed between the host star metallicity (Santos et al. 2001, 2004; Valenti & Fischer 2005) and the frequency of giant planets appears to almost vanish when dealing with these less massive planets (Udry et al. 2006; Sousa et al. 2008, 2011; Mayor et al. 2011; Adibekyan et al. 2012c; Buchhave et al. 2012). In addition, most of Neptune and super-Earth-like planets are found in multiplanetary systems (see e.g. Mayor et al. 2009). Mayor et al. (2011) have recently announced the discovery of 41 planets with HARPS, among which there are 16 super-Earth-like planets. Many of these planets belong to complex planetary systems with a variety of planet masses and orbital properties (see e.g. Lovis et al. 2011), thus challenging our understanding of planet formation and evolution.

The search for peculiarities in the chemical abundance patterns of planet-host stars has also been done (see e.g. Gilli et al. 2006; Ecuivillon et al. 2006; Neves et al. 2009; Adibekyan et al. 2012b), it suggests that there are only small differences in some element abundance ratios between “single” stars (hereafter, “sin-

[★] Based on observations collected with the HARPS spectrograph at the 3.6-m telescope (072.C-0488(E)), installed at the La Silla Observatory, ESO (Chile), with the UVES spectrograph at the 8-m Very Large Telescope (VLT) (program IDs: 67.C-0206(A), 074.C-0134(A), 075.D-0453(A)), installed at the Cerro Paranal Observatory, ESO (Chile), and with the UES spectrograph at the 4.2-m William Herschel Telescope (WHT), installed at the Spanish Observatorio del Roque de los Muchachos of the Instituto de Astrofísica de Canarias, on the island of La Palma

gle” refers to stars without detected planets) and planet hosts (see the introduction in González Hernández et al. 2010, for a more detailed background). However, based on HARPS and Kepler data, Adibekyan et al. (2012a,b) have found that planet-host stars show significant enhancement of alpha elements at metallicities slightly below solar and that they belong to the Galactic thick disk. They find that at metallicities $[\text{Fe}/\text{H}] < -0.3$ dex, 13 planet hosts (HARPS and Kepler samples) out of 17 (about 76 %) are enhanced in alpha elements, while only 32 % of the stars without known planets are alpha-enhanced at a given metallicity. Thus, planet formation requires a certain amount of metals, and therefore, at the relatively low metallicity of $[\text{Fe}/\text{H}] < -0.3$ dex, planet-host stars tend to be alpha-enhanced and tend to belong to the chemically defined thick disk where the stars should have higher overall metallicity (Adibekyan et al. 2012a). This result may be supported by theoretical studies based on core-accretion models (see e.g. Mordasini et al. 2012).

Recently, Meléndez et al. (2009) have found an anomalous but small (~ 0.1 dex) volatile-to-refractory abundance ratio of a sample of 11 solar twins when compared to the solar ratio. They interpret this particularity as a signature of terrestrial planets in the solar planetary system. Their study used high-S/N and high-resolution spectroscopic data. Later on, this conclusion was also supported by Ramírez et al. (2009), who analyzed a sample of 64 solar analogs, but their result was not so evident, at least, not at the level of the accuracy of the abundance pattern shown in Meléndez et al. (2009), where the element abundances are at a distance of ≤ 0.015 dex from the mean abundance pattern (see also Ramírez et al. 2010; Schuler et al. 2011a). González Hernández et al. (2010) analyzed a sample of seven solar twins, five without and two with planets, using very high-quality HARPS spectroscopic data, but maybe still not enough to confirm the result by Meléndez et al. (2009). However, González Hernández et al. (2010) find that on average both stars with and without detected planets seem to exhibit a very similar abundance pattern, even when considering a metal-rich subsample of 14 planet hosts and 14 solar analogs. It is important to note that González Hernández et al. (2010) analyzed stars with planets of different minimum masses from Jupiter-mass to super-Earth planets. Nevertheless, the sample in Ramírez et al. (2009) contains same planet-host stars, but these authors did not distinguish and/or mention them, which may lead to confusing results. The results found by Meléndez et al. (2009) have not been fully confirmed (see also Ramírez et al. 2010; González Hernández et al. 2011a; Gonzalez et al. 2010; Gonzalez 2011; Schuler et al. 2011b), in particular the relation with the presence of planets is strongly debated (González Hernández et al. 2010, 2011b). Recently, they have however found a similar abundance pattern in the solar twin HIP 56948, which they claim may have terrestrial planets (Meléndez et al. 2012).

Delgado Mena et al. (2010) have shown that the chemical abundance pattern of the planet-host stars can be used to distinguish among the different compositions of the possible terrestrial planets. In fact, theoretical simulations based on the observed variations in the chemical abundances of host stars predict diverse compositions for extrasolar terrestrial planets, which are indeed quite different from those of the solar planetary system (Carter-Bond et al. 2012a).

In this paper, we investigate in detail the chemical abundances of “hot” analogs (hereafter, “hot” analogs refers to late F- and early G-type main-sequence stars hotter than the Sun, at temperatures $T_{\text{eff}} \sim 6175$ K) of the HARPS GTO sample, which have narrower convective zones than Sun-like stars, with the aim

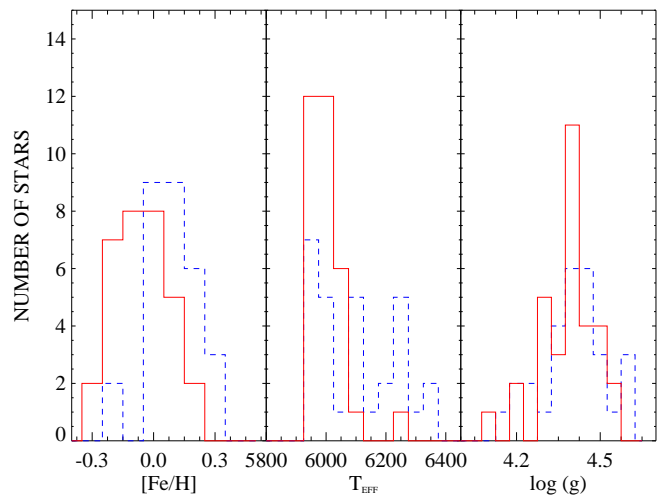


Fig. 1. Histograms of the stellar parameters and metallicities of the whole sample of “hot” analogs hosting planets (blue dashed lines) and without known planets (red solid lines).

Table 2. Ranges of stellar parameters and metallicities in different samples

Sample ^a	T_{eff}	$\log g$	$[\text{Fe}/\text{H}]$	N_{stars}^b
	[K]	[dex]	[dex]	
HA	5950–6400	4.14–4.60	-0.30 – +0.35	61
mrHA	5950–6400	4.14–4.60	+0.04 – +0.19	26

Notes. ^(a) Stellar samples: “hot” analogs, “HA”, metal-rich “hot” analogs, “mrHA”. ^(b) Total number of stars including those with and without known planets.

of searching for the enhanced signature of terrestrial planets in their abundance patterns. We also reanalyzed the data of the solar analogs presented in González Hernández et al. (2010) taking the new discovered planets into account (see e.g. Mayor et al. 2011). We pay special attention to eight solar analogs harboring super-Earth-like planets under the assumption that these small planets may have similar chemical composition to that of terrestrial or Earth-like planets.

2. Observations

In this study, as in González Hernández et al. (2010), we analyze high-resolution and high-S/N spectroscopic data obtained with three different telescopes and instruments: the 3.6m-ESO/HARPS at the *Observatorio de La Silla* in Chile, the 8.2m-VLT/UVES at the *Observatorio Cerro Paranal* in Chile, and the 4.2m-WHT/UES at the *Observatorio del Roque de los Muchachos* in La Palma, Spain. In Table 1, we provide the wavelength ranges, resolving power, S/N, and other details of these spectroscopic data. The data were reduced in a standard manner and later normalized within the package IRAF¹, using low-order polynomial fits to the observed continuum.

¹ IRAF is distributed by the National Optical Observatory, which is operated by the Association of Universities for Research in Astronomy, Inc., under contract with the National Science Foundation.

Table 1. Spectroscopic observations

Spectrograph	Telescope	Spectral range	$\lambda/\delta\lambda$	Binning	N_{stars}^a	S/N ^b	δ S/N ^c	Δ S/N ^d
		[Å]		[Å/pixel]				
HARPS	3.6m-ESO	3800–6900	110,000	0.010	50	877	429	265–2015
UVES	8m-VLT	4800–6800	85,000	0.016	7	722	150	510–940
UES	4.2m-WHT	4150–7950	65,000	0.029	4	643	180	520–850

Notes. Details of the spectroscopic data used in this work. The UVES and UES stars are all planet hosts. Three of the UVES stars were observed with a slit of 0.3'' providing a resolving power $\lambda/\delta\lambda \sim 110,000$. ^(a) Total number of stars including those with and without known planets. ^(b) Mean signal-to-noise ratio, at $\lambda = 6070$ Å, of the spectroscopic data used in this work. ^(c) Standard deviation from the mean signal-to-noise ratio. ^(d) Signal-to-noise range of the spectroscopic data.

Table 3. Stellar parameters and metallicities from the UVES and UES spectra

HD	T_{eff}	δT_{eff}	$\log g$	$\delta \log g$	ξ_t	$\delta \xi_t$	[Fe/H]	δ [Fe/H]
	[K]	[K]	[dex]	[dex]	[km s ⁻¹]	[km s ⁻¹]	[dex]	[dex]
209458 ^a	6118	22	4.50	0.04	1.21	0.03	0.03	0.02
2039 ^a	5959	31	4.45	0.04	1.26	0.03	0.32	0.02
213240	6022	19	4.27	0.05	1.25	0.02	0.14	0.01
23596 ^b	6134	35	4.25	0.08	1.30	0.04	0.31	0.03
33636	5994	17	4.71	0.02	1.79	0.02	-0.08	0.01
50554 ^b	6129	50	4.41	0.07	1.11	0.06	0.01	0.04
52265 ^a	6136	46	4.36	0.04	1.32	0.06	0.21	0.03
72659	5951	13	4.30	0.02	1.42	0.01	0.03	0.01
74156	6099	19	4.34	0.03	1.38	0.02	0.16	0.01
89744 ^b	6349	43	3.98	0.05	1.62	0.05	0.22	0.03
9826 ^b	6292	43	4.26	0.06	1.69	0.05	0.13	0.03

Notes. Stellar parameters, T_{eff} and $\log(g/\text{cm s}^2)$, microturbulent velocities, ξ_t , and metallicities, [Fe/H], and their uncertainties, of the planet-host stars observed with UVES/VLT and UES/WHT spectrographs.

^(a) Stars observed with the UVES spectrograph at VLT telescope at $\lambda/\delta\lambda \sim 110,000$. The other stars were observed with UVES at $\lambda/\delta\lambda \sim 85,000$.

^(b) Stars observed with the UES spectrograph at WHT telescope at $\lambda/\delta\lambda \sim 65,000$.

3. Sample

With the aim of performing a detailed chemical analysis, we selected late F- and early G-type stars with spectra at S/N > 250 from these three spectrographs. We end up with a sample of 29 planet-host stars and 32 “single” stars (see Fig. 1). All UVES and UES stars are planet hosts. In Table 2 we provide the ranges of stellar parameters and metallicities of the 61 “hot” analogs of the sample. In Fig. 1, we display the histograms of the effective temperatures, surface gravities, and metallicities of this sample. The stars hosting planets are on average more metal-rich than the stars without planets. Thus, we define a subsample of metal-rich late F- and early G-type stars with $0.04 < [\text{Fe}/\text{H}] < 0.19$, containing 13 planet hosts and 13 “single” stars (see Table 2). On the other hand, due to the recently discovered new planets (see e.g. Mayor et al. 2011) in the sample of solar analogs presented in González Hernández et al. (2010), there are now 33 stars with planets and 62 stars without planets.

4. Stellar parameters

The stellar parameters and metallicities of the HARPS stars were extracted from the work by Sousa et al. (2008), which are based on the equivalent widths (EWs) of 263 Fe I and 36 Fe II lines,

measured with the code ARES² (Sousa et al. 2007) and which evaluates the excitation and ionization equilibria. For the UVES and UES stars we decided to recompute the stellar parameters (see Table 3) using these higher quality data. Chemical abundances of Fe lines were derived using the 2002 version of the LTE code MOOG (Snedden 1973), and a grid of Kurucz ATLAS9 plane-parallel model atmospheres (Kurucz 1993).

5. Chemical abundances

We performed a fully differential analysis that is, at least, internally consistent. Thus, we used the HARPS solar spectrum³ of the *Ganymede*, a *Jupiter*’s satellite, as solar reference (see González Hernández et al. 2010). We note here that the UVES and UES stars were also analyzed using the HARPS *Ganymede* spectrum as solar reference owing to the lack of an appropriate solar spectrum observed with these two instruments.

We computed the EW of each spectral line using the code ARES (Sousa et al. 2007) for most of the elements. However, as in González Hernández et al. (2010), for O, S, and Eu, we

² The ARES code can be downloaded at <http://www.astro.up.pt/>

³ The HARPS solar spectrum can be downloaded at <http://www.eso.org/sci/facilities/lasilla/instruments/harps/inst/monitoring/sun.html>

calculated the EW by integrating the line flux and for Zr, by performing a Gaussian fit taking into account possible blends. In both cases, we use the task `SPLIT` within the IRAF package. The EWs of Sr, Ba, and Zn lines were checked within IRAF, because, as for the elements O, S, Eu, and Zr, for some stars, ARES did not find a good fit due to numerical problems and/or bad continuum location. For further details see Sect. 5 in González Hernández et al. (2010).

The oxygen abundance was derived from the forbidden [O I] line. This line is severely blended with a Ni I line (see e.g. Allende Prieto et al. 2001). We adopted the atomic parameters for the Ni line from Allende Prieto et al. (2001) and for [O I] line from Lambert (1978). For more details see Ecuivillon et al. (2006). We derived the EW of Ni line using the mean Ni abundance of the star and subtracted this EW from the overall EW of the [O I] feature. The remaining EW value give us the O abundance of the star. In the solar case, the atlas solar spectrum (Kurucz et al. 1984), the whole feature has an EW of ~ 5.4 mÅ, which provides an abundance⁴ of $A(O) = 8.74$ dex (see González Hernández et al. 2010, for more details).

We again used MOOG (Snedden 1973) and ATLAS models (Kurucz 1993) to derive the abundance of each line and thus determined the mean abundance of each element relative to its solar abundance on a line-by-line basis. However, to avoid problems with incorrect EW measurements of some spectral lines, we rejected all the lines with a different abundance from the mean abundance by more than a factor of 1.5 times the rms. We also checked that we get the same results when using a factor of 2 times the rms, but we decided to stay in a more restrictive position. For 34 F- and G-type stars without planets in our sample, the line-by-line scatter in the differential abundances goes on average from $\sigma \sim 0.014 - 0.025$ for elements such as Si, Ni, Cr, Ca, and Ti, to $\sigma \sim 0.035$ for C and Sc, to $\sigma \sim 0.050$ for Mg and Na, and to $\sigma \sim 0.063$ for S. These numbers are comparable to those found in solar analogs (see González Hernández et al. 2010).

6. Discussion

In this section we inspect the abundance ratios of different elements as a function of the metallicity, [Fe/H], as well as the relation, for different samples of “hot” analogs, between the abundance difference, $\Delta[X/Fe]_{\text{SUN-STAR}}$, and the 50% equilibrium condensation temperature, T_C (see Lodders 2003). We also explore the abundance pattern of some particular stars containing super-Earth-like planets in the sample of both “hot” analogs and solar analogs.

6.1. Galactic abundance trends

In Figs. 2, and 3 we depict the very accurate abundance ratios [X/Fe] of many elements in this sample of late F- and early G-type stars with and without planets, derived from the high-quality HARPS, UVES, and UES spectra. These Galactic trends are compatible with those of Galactic thin disk stars (see e.g. Bensby et al. 2005; Reddy et al. 2006; Gilli et al. 2006; Takeda 2007; Neves et al. 2009; Delgado Mena et al. 2010; Adibekyan et al. 2012c) and, in particular, with those of solar analogs (Ramírez et al. 2009; González Hernández et al. 2010). We may note the small differences in the fits to the abundances of the “single” “hot” analogs and “single” solar analogs. In particular, the element O reveals slight differences at the lowest metal-

licities (i.e. at [Fe/H] ~ -0.3 in this sample) whereas Mn, Co, Sr, Ba, Ce and Nd present these small differences at the highest metallicities (i.e. at [Fe/H] $\sim +0.3$ in this sample). There is also a tiny shift of $\sim 0.03 - 0.05$ in the fits of Al and V. However, in general for the rest of the elements like S, Si, Ca, Ti, Cr, and Ni, we almost find perfect agreement. In Tables A.1–A.8, we provide the element abundance ratios [X/Fe] which are all available online⁵.

6.2. Mean abundance ratios [X/Fe] versus T_C : previous results

Meléndez et al. (2009) suggest that the formation of rocky planets in the solar system affects the composition of solar photosphere by lowering the amount of refractory elements with respect to the volatile elements. They focus on Earth-like planets and do not comment on how much the formation of other slightly more massive planets like super-Earth- and Neptune-like planets would affect their interpretation of the mean abundance pattern of solar twins with respect to the Sun.

According to the element abundances of the Earth (Kargel & Lewis 1993), the bulk composition of a terrestrial planet should be dominated by O, Fe, Mg, and Si, with small amounts of Ca and Al and with very little C. These terrestrial planets would be composed by Mg silicates and metallic Fe, with other species present in relatively minor amounts. Water and other hydrous phases may or may not be present (Bond et al. 2010). The composition of Earth-like planets depends on the chemical composition of the host star (Bond et al. 2010; Carter-Bond et al. 2012a; Delgado Mena et al. 2010), and a wide variety of terrestrial planets compositions is predicted. Also giant planet migration plays an important role in the final Earth-like compositions (Carter-Bond et al. 2012b). A variation of $\pm 25\%$ from the Earth composition should be considered to include Venus and Mars as terrestrial planets (Carter-Bond et al. 2012a).

Depending of the final compositions, these Earth-like planets could have substantial amounts of water and develop plate tectonics (Carter-Bond et al. 2012b), which have been proposed as necessary conditions for life. Simulations of super-Earth-like planets reveal that these slightly more massive planets could also have plate tectonics (Valencia et al. 2007a). These authors consider unlikely, although possible, that super-Earth-like planets could have a lot of gas (Valencia et al. 2007b), as they state that at higher masses than $10 M_{\oplus}$, there is a possibility that H and He are retained, although these could give rise to massive ocean planets with high H₂O content and a relatively small layer of gas above it (Valencia et al. 2007b). We should note, however, that these simulations of super-Earth-like planets assumed a given planetary composition similar to Earth-like planets, but it seems reasonable to assume that super-Earth-like planets, since formed in the same protoplanetary disk, could become a larger counterpart of Earth-like planets and therefore have a similar composition.

Ramírez et al. (2009) derived the slopes of trends described by the abundance ratios of a sample of solar analogs versus the condensation temperature, T_C . Although they only took those elements with $T_C > 900$ K into account, they argue that, following the reasoning in Meléndez et al. (2009), a negative slope is an indication that a star should not have terrestrial planets even if

⁵ The online Tables A.1–A.8 are available in electronic form at the CDS via anonymous ftp to cdsarc.u-strasbg.fr (130.79.128.5) or via <http://cdsarc.u-strasbg.fr/viz-bin/qcat?J/A+A/...>

⁴ $A(X) = \log[N(X)/N(H)] + 12$

this star already contains giant planets. We note in this paper, as in González Hernández et al. (2010), that we are evaluating the abundance differences $\Delta[X/Fe]_{\text{SUN-STARS}}$, and thus we follow the same reasoning as in Meléndez et al. (2009). These authors also analyze ten solar analogs, among which four have close-in giant planets. Their abundance pattern differs from the Sun's but resembles that of their solar twins. Although the result was statistically not significant, they suggest that stars with and without close-in giant planets should reveal different abundance patterns.

González Hernández et al. (2010) studied the abundance trends of solar analogs with and without planets and find that most of these stars have negative slopes, hence indicating that these stars should not contain terrestrial planets. Two stars in their sample with super-Earth-like planets, HD 1461 and HD 160691, provide abundance trends $[X/Fe]_{\text{SUN-STARS}}$ versus condensation temperature, T_C , with the opposite slope to what is expected if these stars contain terrestrial planets. Therefore, González Hernández et al. (2010) suggest that these abundance patterns are not related to the presence of terrestrial planets. They also note that the abundance patterns of solar analogs are strongly affected by chemical evolution effects, especially for elements with steep Galactic trends like Mn (with $T_C \sim 1160$ K).

Ramírez et al. (2010) combined chemical abundance data of solar analogs from previous studies. They produce an average abundance pattern consistent with their expectations (Ramírez et al. 2009) but extracted from more noisy abundance patterns. They also argue that when deriving the slopes for elements with $T_C > 900$ K in the two planet hosts HD 1461 and HD 160691, they obtained the sign consistent with the results by Ramírez et al. (2009). González Hernández et al. (2011b) demonstrate instead that using the elements $T_C > 1200$ K provides the opposite sign as in the case of $T_C > 900$ K. Unfortunately, there are more refractory elements, most of them with $T_C > 1200$ K, than volatile elements. Thus a more reliable trend should consider the whole range of T_C values for the available elements, i.e. $0 < T_C < 1800$ K (González Hernández et al. 2011b). In addition, subtracting the Galactic chemical evolution effects before fitting the abundance ratio $[X/Fe]$ almost completely removes any trend not from these two planet-host stars but also from the average values of the subsample of metal-rich solar analogs (González Hernández et al. 2011a).

Gonzalez et al. (2010) and Gonzalez (2011) investigated the abundances of refractory and volatile elements in a smaller sample of stars with and without giant planets. They claim to confirm the results by Ramírez et al. (2009) but in a broader effective temperature, T_{eff} , range. They also state that more metal-rich stars display steeper trends than more metal-poor counterparts. Schuler et al. (2011b) analyzed a small sample of ten stars known to host giant planets using very high-S/N and very high-resolution spectra but in the wide T_{eff} range 5600–6200 K and in the metallicity, $[Fe/H]$, range 0–0.4 dex. They chose instead to fit the abundances $[X/H]$ versus T_C and found positive slopes in four stars with close-in giant planets and flat or negative slopes in stars with planets at longer orbital periods, thus consistent with recent suggestions of the terrestrial planet formation signature. They contend, however, that these trends probably result from Galactic chemical evolution effects.

More recently, Schuler et al. (2011a) and Ramírez et al. (2011) have presented a detailed chemical analysis of the two solar twins of the 16 Cygni binary system. One of them, 16 Cygni B contains a Jupiter-mass planet in an eccentric orbit, but no planet has been detected around 16 Cygni A. According to Schuler et al. (2011a), these two stars appear to be chemically identical, with a mean difference of 0.003 ± 0.015 dex. On the

other hand, Ramírez et al. (2011) find that star A is more metal-rich than star B by 0.041 ± 0.007 dex, and suggested that this may be related to the formation of giant planet in star B. Both results may be consistent at the $3\text{-}\sigma$ level and probably indicate that internal systematics are greater than typically assumed. Takeda (2005) claims there is no metallicity difference between 16 Cygni A and B. Laws & Gonzalez (2001) were the first in performing a differential analysis and they also suggest that star A is more metal-rich than star B by 0.025 ± 0.009 dex, but only based on the analysis of iron lines.

6.3. All “hot” analogs

The whole sample of stars presented in this work is composed of 61 late F- and early G-type stars, 29 planet hosts, and 32 “single” stars. In Fig. 4 we display the mean abundance difference, $\Delta[X/Fe]_{\text{SUN-STARS}}$, versus the condensation temperature, T_C , using the HARPS spectrum⁶ of *Ganymede* as solar reference (see González Hernández et al. 2010, for further details). The left panel of Fig. 4 evokes high scatter among the points for different elements for stars both with and without planets, and therefore the fits are very tentative and do not provide any additional information. However, that in this relatively narrow metallicity range the Galactic trends shown in Figs. 2, and 3 give different slopes, strongly affects the mean element abundance ratios. For this reason, we also computed the values $\Delta[X/Fe]_{\text{SUN-STARS}}$ but after subtracting these Galactic evolution effects. To do that, we fit a linear function to the Galactic trends of the 32 “hot” analogs without planets (see linear fits in Figs. 2, and 3) and subtracted the value given by this fit at the metallicity of each star to the abundance ratio of the star.

The result is depicted in the right-hand panel of Fig. 4. For “single” stars, the mean abundance ratios of practically all elements roughly become zero, with a tiny scatter ($\sigma = 0.0097$), as well as the slope of the fit to all mean abundances is almost zero, with a value of $(-0.09 \pm 0.04) \times 10^{-4}$ dex K^{-1} . For “hot” analogs hosting planets, the remaining scatter is larger, so the slope of the fit remains negative, $(-0.24 \pm 0.05) \times 10^{-4}$ dex K^{-1} (see Table 4). This is probably because we are using the linear fits to the Galactic trends of stars without planets, although the abundance ratios of planet hosts seem to follow the Galactic trends defined by these linear fits. However, if we choose planet hosts to fit their galactic chemical trends the result give a similar scatter ($\sigma = 0.0121$) as the that that abundance ratios of “single” stars in Fig. 4, and the fit is close to zero (-0.013 ± 0.046). Hereafter we use abundance ratios of “single” stars to fit the Galactic trends because they cover the whole range of metallicity, whereas planet hosts mostly cover metallicities $[Fe/H] > 0$, thus “single” stars are better tracers of Galactic chemical evolution effects.

This may be also due to intrinsic differences between the abundance pattern of stars with and without planets, a possibility that we explore in Section 6.7. This could be also related to the different metallicity distributions of stars with and without planets, where the former is more metal-rich, but as we see in Section 6.4, a subsample of metal-rich “hot” analogs without planets still behaves in a different way than a similar sample of stars with planets.

⁶ The HARPS solar spectra can be downloaded at <http://www.eso.org/sci/facilities/lasilla/instruments/harps/inst/monitoring/sun.html>

Table 4. Slopes of the linear fit to the mean values $\Delta[X/Fe]_{\text{SUN-STARS}}$ versus T_C

Sample ^a	Non-GCE ^b	GCE ^b	N_{stars}^c
sSA	-0.378 ± 0.033	-0.060 ± 0.029	62
pSA	-0.302 ± 0.047	$+0.014 \pm 0.040$	33
smrSA	-0.235 ± 0.055	-0.062 ± 0.053	16
pmrSA	-0.194 ± 0.048	-0.027 ± 0.047	16
sHA	-0.160 ± 0.046	-0.086 ± 0.041	32
pHA	-0.404 ± 0.048	-0.242 ± 0.046	29
smrHA	-0.111 ± 0.062	-0.106 ± 0.061	13
pmrHA	-0.506 ± 0.066	-0.379 ± 0.063	13
smrHAh	-0.330 ± 0.069	-0.258 ± 0.070	10
pmrHAh	-0.419 ± 0.068	-0.289 ± 0.067	10
pSAlp	-0.099 ± 0.067	$+0.125 \pm 0.059$	13
pSAmp	-0.370 ± 0.075	-0.044 ± 0.062	14
pSAsp	-0.404 ± 0.114	-0.103 ± 0.092	6
pSAlm	-0.348 ± 0.059	-0.077 ± 0.050	21
pSAm	$+0.236 \pm 0.114$	$+0.383 \pm 0.097$	4
pSAsm	-0.223 ± 0.084	$+0.199 \pm 0.065$	8

Notes. Slopes of the linear fit of the mean abundance ratios, $\Delta[X/Fe]_{\text{SUN-STARS}}$, as a function of the condensation temperature, T_C , using the whole T_C interval, for different stellar samples. ^(a) Stellar samples: “single” solar analogs, “sSA”, planet-host solar analogs, “pSA”, “single” metal-rich solar analogs, “smrSA”, planet-host metal-rich solar analogs, “pmrSA”. “HA” refers to “hot” analogs and “HAh” refers to very high S/N data (S/N > 550). Planet-host solar analogs with the most massive planet in an orbital period $P_{\text{orb}} < 25$ days, “pSAsp”, $100 < P_{\text{orb}} < 600$ days, “pSAmp”, $900 < P_{\text{orb}} < 4250$ days, “pSAlp”. Planet-host solar analogs with the minimum mass, $m_p \sin i$, of the least massive planet in the ranges: $m_p < 14 M_{\oplus}$, “pSAsm”, $14 < m_p < 30 M_{\oplus}$, “pSAm”, $m_p > 30 M_{\oplus}$, “pSAlm”. ^(b) “Non-GCE” and “GCE” refers to the mean abundances before and after being corrected for galactic chemical evolution effects. ^(c) Total number of stars in the sample.

6.4. Metal-rich “hot” analogs

We selected a subsample of 26 metal-rich “hot” analogs with the aim of investigating the abundance pattern of similar samples of stars with and without planets with very similar metallicity distribution. Thus, we selected 13 planet-host and 13 “single” late F- and early G-type stars. In Fig. 5 we display the mean values $\Delta[X/Fe]_{\text{SUN-STARS}}$ for these two subsamples. In the left-hand panel of Fig. 5, planet hosts again yield a steeper abundance trend versus condensation temperature than “single” hot analogs. However, in the right-hand panel of Fig. 5, after removing the chemical evolution effects, the abundance pattern of “single” stars does not exhibit any trend whereas for planet hosts the mean abundances still hold a negative slope.

Meléndez et al. (2009), González et al. (2010), and González (2011) found that the planet-host stars show steeper trends than “single” stars at high metallicity although this effect is probably related to chemical evolution effects. González Hernández et al. (2011a) depicted in their Fig. 3 the mean abundance trends of a subsample of metal-rich solar analogs with and without planets together with steep fits to the data, but with similar slopes in both cases, $(-0.23 \pm 0.06) \times 10^{-4}$ dex K^{-1} for “single” stars and $(-0.16 \pm 0.05) \times 10^{-4}$ dex K^{-1} for planet-host stars (see also González Hernández et al. 2010). They display in their Fig. 4 however that after removing the galactic chemical evolution effects, these negative trends almost disappear, and clearly the

slopes of stars with and without planets are consistent within the $1\text{-}\sigma$ uncertainties, $(-0.07 \pm 0.06) \times 10^{-4}$ dex K^{-1} for “single” stars and $(-0.02 \pm 0.05) \times 10^{-4}$ dex K^{-1} for planet-host stars (see Table 4). In addition, the mean abundance pattern of solar analogs after correcting for galactic chemical evolution also exhibit flat trends for the 62 “single” stars and 33 planet hosts (González Hernández et al. 2013b). On the other hand, if one chooses a subsample of very high-quality spectra of metal-rich “hot” analogs with S/N > 550, then although the trends still remain very steep with negative slopes, in this case, for ten stars with and ten without planets (González Hernández et al. 2013a), these slopes are both very similar and consistent within the error bars (see Table 4).

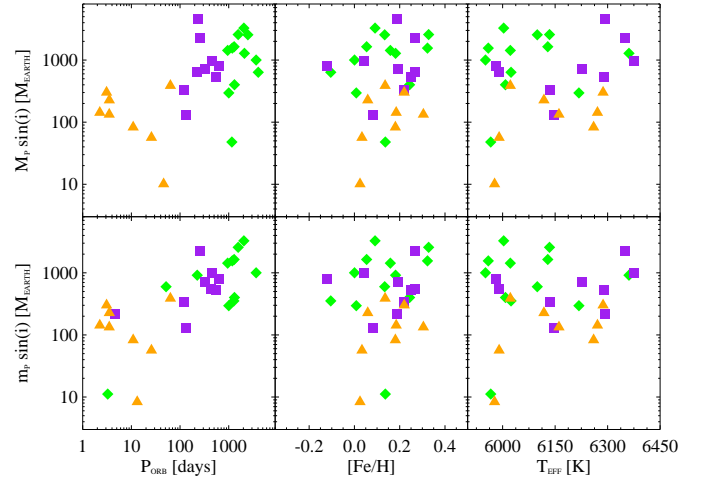


Fig. 8. Top panels: Minimum mass of the most massive planet of each of “hot” analogs hosting planets versus the orbital period of the planet (left panel) and metallicity [Fe/H] (middle panel), and temperature (right panel), with the most massive planet in an orbital period $P_{\text{orb}} < 65$ days (diamonds), $115 < P_{\text{orb}} < 630$ days (squares), $950 < P_{\text{orb}} < 4050$ days (triangles). Bottom panels: the same as top panels but showing the minimum mass of the least massive planet. The symbols as in top panel.

6.5. Revisiting solar analogs

The number of planet hosts in the sample of solar analogs in González Hernández et al. (2010) have changed due to the discovery of planets of different masses, in particular, low-mass planets with masses below $30 M_{\oplus}$ (see e.g. Mayor et al. 2011). We have reanalyzed the data presented in González Hernández et al. (2010) and been able to correct the abundance differences, $\Delta[X/Fe]_{\text{SUN-STARS}}$, for the chemical evolution effects using the linear fits to the Galactic abundance ratios, $[X/Fe]$, of solar analogs without known planets.

In Fig. 6 we display the mean abundance differences for updated lists of stars with and without detected planets. Stars hosting planets are also separated for different orbital periods of the most massive planet in the planetary systems. However, we do not see any clear signature. All of them show similar mean abundance pattern although with slightly different slopes, to those found for the whole samples of stars with and without planets. However, one could speculate that the positive trend seen for the largest orbital periods ($P_{\text{orb}} > 900$ days) would allow the formation of terrestrial planets in closer orbits. For the most massive

planets at the orbital periods between 100 and 600 days, we get a flat trend (see Table 4). The stars with the most massive planets at the shortest periods ($P_{\text{orb}} < 25$ days) display a slightly negative trend, which would indicate that these stars would not have formed terrestrial planets or that they have been captured via, for instance, a possible inward migration of the most massive planets in these systems. A similar slope is found for stars without detected planets; however, these slope values are only significant at $\leq 2 \sigma$ (see Table 4), which probably makes the previous statement too tentative.

In the right-hand panel of Fig. 6, we depict the mean abundance differences but separate the planet hosts into several ranges of the minimum mass of the least massive planet. The mean abundance patterns are similar, but the slopes of the trends seem to behave in different ways depending on the range of masses. We again try to speculate on these results to try to identify possible explanations. The stars containing super-Earth-like planets show an increasing trend, which would indicate that these stars are slightly different from the Sun and that the super-Earth-like planets behave on average like the terrestrial planets of the solar planetary system, but with higher amount of metals trapped on these super-Earth-like planets. On the other hand, the stars harboring Neptune-like planets show on average a steep positive trend slope that would mean that the Neptune-like planets have, as one may expect, a higher content of refractory elements than the Sun and that the volatile content caught in Neptune-like planets would not be too large. Finally, the stars hosting Jovian planets exhibit a slightly negative or almost flat trend, which may indicate that these stars only harbor giant planets, although in that case one would expect to see a steep negative trend. The possibility still remains that these stars harbor a small number of terrestrial planets. The ideal situation would be to group the stars taking the planet mass and periods into account at the same time but the statistics would be even worse. Thus, although these statements appear to follow the line of reasoning in Meléndez et al. (2009), we think we need more Sun-like stars with already detected planets at different masses and orbital periods and with high-quality data to confirm this very tentative scenario. In the next section we individually inspect the abundance pattern of the stars hosting super-Earth-like and Neptune-like planets to try to elucidate whether there is a connection between the amount of rocky material in the low-mass planets and the slopes of the abundance trends of each star.

6.6. Stars hosting super-Earth-like planets

González Hernández et al. (2010) already studied the abundance trends of two stars in their sample, with negative slopes, which harbor super-Earth-like planets, HD 1461 and HD 160691. Taking into account the new discovered planets presented e.g. in Mayor et al. (2011), our sample of solar analogs analyzed in González Hernández et al. (2010) and our sample of “hot” analogs now contain 8 and 2 stars hosting super-Earth-like planets, respectively. It is therefore interesting to look at the abundance pattern of these stars harboring, at least, super-Earth-like planets under the assumption that these exoplanets contain a significant amount of rocky material in the form of refractory elements. We note here that the masses of the planet are indeed minimum masses, so that in some cases the “real” planet mass could be significantly higher. However, statistical analysis show that the distribution of $m_p \sin i$ values is similar to that of “ m_p ” values (Jorissen et al. 2001). In fact, the average value of $\sin i$ for a random distribution of angles is of 0.79, so the average factor of overestimation is only 1.27.

In Fig. 7 we display the abundance pattern of ten stars hosting super-Earth-like planets in the sample of “hot” analogs and the sample of solar analogs analyzed in González Hernández et al. (2010). The abundance differences of these stars, $\Delta[X/\text{Fe}]_{\text{SUN-STARS}}$, are plotted versus the condensation temperature, T_C . The abundances ratios of each star were corrected for the Galactic trends at the metallicity of the star. To compute these abundance corrections, we used the linear fitting functions of the galactic abundances of both the sample of 32 “hot” and 62 solar analogs without detected planets. In Fig. 7 we also show the fits to all abundance ratios of each star weighted by their uncertainties. There are many more refractory elements (with $T_C \gtrsim 1200$ K) than volatile elements, so a more reliable fit of these element abundance ratios should consider all of the T_C values. However, we still find that this fitting procedure does not give the same weight to all T_C values and thus we decided to average the abundance ratios in bins of $\Delta T_C = 150$ K. We estimate the error bars of these new points as the maximum value between standard deviation from the mean abundance and the mean abundance uncertainty of the elements at each T_C bin, unless there is only one point in this T_C bin, in which case, the error bar is associated with the abundance uncertainty of the given element. The error bar is estimated in this way in order to consider all possible sources of uncertainty, i.e. not only the scatter of the element abundances but also the individual abundance uncertainties. These new data points are also depicted in Fig. 7, together with their corresponding linear fitting functions, which were again derived by the fit of these points weighted by their error bars. The slope of these linear fits is our adopted slope to be evaluated in the context of the possible presence of terrestrial planets in these stars. In many cases, these new fits of the average points are similar to those corresponding to the individual element abundances.

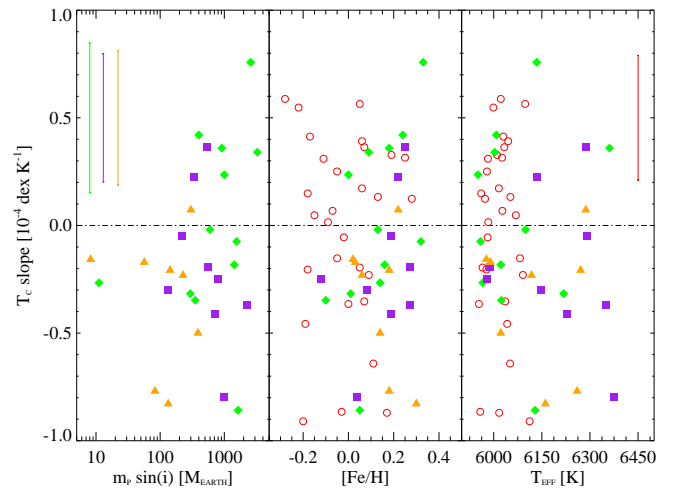


Fig. 9. Slopes of the linear fits to 61 “hot” analogs of the mean element abundance ratios, $\Delta[X/\text{Fe}]_{\text{SUN-STARS}}$, versus the condensation temperature, T_C , as a function of the minimum mass of the least massive planet of each planet-host star (left panel), the stellar metallicity (middle panel), and effective temperature (right panel). The mean error bars of the slopes are shown in upper-left corner for planet hosts and upper-right corner for “single” stars. The symbols as in Fig. 8.

By inspecting Fig. 7, one realizes that there are four stars showing positive slopes, three showing negative slopes, and

three giving a flat slope. We note that if all the stars provided a flat slope, the interpretation related to the existence of terrestrial planets would lose its meaning. Either way, the magnitude of the slope should be related to the amount of rocky material present in these planetary systems. Thus, finding one single planetary system that does not accomplish the expected slope may be enough to rule out the statement claiming that the abundance pattern of a star conceals a signature of rocky planets. In these small subsamples of ten stars hosting small planets, there are three stars providing negative trends, but having relatively massive super-Earth-like planets. In these three stars, one would expect to find, at least, similar positive trends. However, we still do not know if these stars actually harbor really rocky Earth-like planets.

In Fig. 7 we also indicate the number of confirmed planets in these planetary systems. There does not seem to be any connection between the number of planets and the slope of the abundance pattern versus condensation temperature. There are solar analogs with only two detected planets, HD 1461 and HD 96700, whose less massive planet have $5.9 M_{\oplus}$ and $9.0 M_{\oplus}$ at orbital periods $P_{\text{orb}} \sim 13.5$ days and 8.1 days, respectively. These two solar analogs also have a second super-Earth-like planet with masses $7.6 M_{\oplus}$ and $12.7 M_{\oplus}$, at $P_{\text{orb}} \sim 5.8$ days and 103.5 days, respectively, hence a significant amount of rocky material. Nevertheless, they both exhibit unexpected, nearly flat trends. In addition, the two “hot” analogs, with $T_{\text{eff}} \sim 5975$ K, should have narrower convective zones than the Sun what would make it easier to detect any possible signature for terrestrial planets. These two stars, HD 93385 and HD 134060, harbor two planets each with masses $8.4 M_{\oplus}$ and $10.2 M_{\oplus}$ (at $P_{\text{orb}} \sim 13.2$ and 46 days) and $11.2 M_{\oplus}$ and $47.9 M_{\oplus}$ (at $P_{\text{orb}} \sim 3.2$ and 1160.9 days). These planets should also contain a large amount of rocky material, hence refractory elements, but they have slightly lower volatile-to-refractory abundance ratios than the Sun, and therefore should have less rocky material than the solar planetary system.

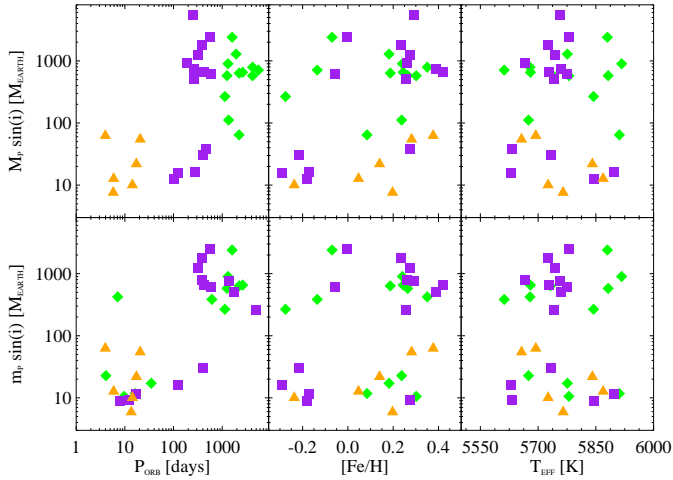


Fig. 10. Same as Fig. 8, but for solar analogs hosting planets, with the most massive planet in an orbital period $P_{\text{orb}} < 25$ days (diamonds), $150 < P_{\text{orb}} < 650$ days (squares), $1000 < P_{\text{orb}} < 4300$ days (triangles).

It is actually plausible that many of our stars in both samples of “hot” and solar analogs host really terrestrial planets. Numerical simulations reveal that low-mass (from Neptune-like to Earth-like) planets are much more common than giant planets,

this effect is more significant as the metallicity decreases, and probably 80–90% of solar-type stars have terrestrial planets (see e.g. Mordasini et al. 2009a,b, 2012). This statement agrees with the growing population of low-mass planets found in the HARPS sample of exoplanets (Udry & Santos 2007; Howard et al. 2010; Mayor et al. 2011).

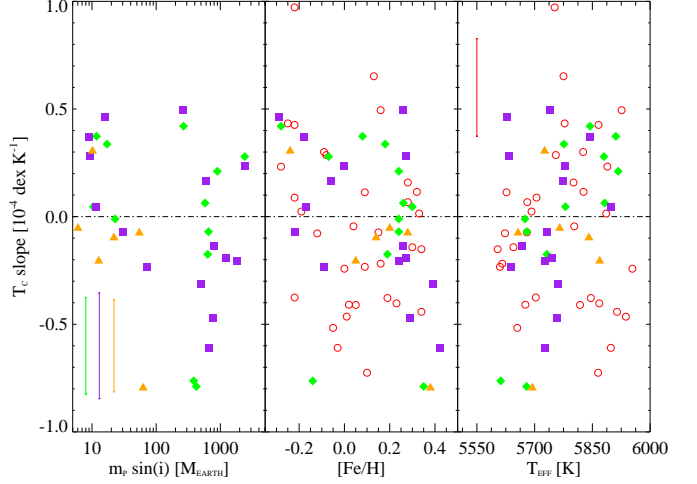


Fig. 11. Same as Fig. 9 but for solar analogs. The symbols as in Fig. 10.

6.7. Planetary signatures in the abundance trends?

We now explore the abundance trends of the whole sample of “hot” and solar analogs to extract information on the amount of rocky material in their planetary systems. In Fig. 8 we depict the important orbital properties, minimum mass of the most massive and the least massive planets, and the orbital period as well as two stellar properties, metallicity, and effective temperature, of all the 29 “hot” analogs with planets. Figure 8 exhibits a variety of planetary systems, many of them with more than one or two planets. This plot also allows us to see that there are only two stars hosting super-Earth-like planets (see also Fig. 7) with $T_{\text{eff}} \sim 5975$ K and metallicities slightly above solar, but also that the most massive planets in these systems are another super-Earth-like and one Saturn-like planet in about 6- and 100-day orbits (see Section 6.6). In Fig. 8 we are also able to distinguish many stars harboring isolated planets with masses between 50 and $3500 M_{\oplus}$. The stellar properties of the stars, T_{eff} and $[\text{Fe}/\text{H}]$, exhibit uniform behavior irrespective for the orbital period of the most and the least massive planets in each planetary system.

Although the planetary systems of the sample of “hot” analogs exhibit a substantial complexity, we try to extract information from the slopes of the average abundances versus the condensation temperature as seen in Section 6.6. Thus we derive the trend in the average abundances in T_C bins of each “hot” analog as shown for the stars hosting super-Earth-like planets in Fig. 7. In Fig. 9 we depict the slopes of these average trends against the minimum mass of the least planet mass, the stellar metallicity, and the effective temperature. We also display the slopes for “hot” analogs without known planets. According to the line of reasoning in Meléndez et al. (2009), positive slopes would mean that these stars are deficient in refractory elements with respect to the Sun and hence likely to host terrestrial planets. From this plot one realizes that only a few stars that al-

ready harbor giant planets would also have terrestrial planets. However, most of the “hot” analogs, in particular two stars that already contains super-Earth-like planets exhibit negative slopes, so have less probability of hosting terrestrial planets. We also include stars without known planets and more than half of them show positive slopes and therefore should have terrestrial planets.

In Fig. 10, we display the minimum masses of the planets orbiting 33 solar analogs similarly as Fig. 8. We notice here that there are eight solar analogs with super-Earth-like planets with masses between $6 M_{\oplus}$ and $13 M_{\oplus}$ at orbital periods between 6 and 16 days, and four Neptune-like planets, with masses $16 M_{\oplus}$ and $23 M_{\oplus}$ at P_{orb} in the range 4–122 days. The distributions of effective temperatures and metallicities among solar analogs are also approximately homogeneous and do not depend on the orbital period of the planets. In Fig. 11, we depict the slopes for solar analogs with and without planets computed as in Fig. 9. We also display the mean error bars for different samples of stars with and without planets to illustrate how accurate these slopes are. In fact, many of these values are consistent with flat slopes. We see that many stars with low-mass planets exhibit positive slopes. Most of these planetary systems have Jupiter-like or Saturn-like planet at orbital periods longer than 100 days. On the other hand, the two solar analogs, showing negative slopes, only harbor super-Earth-like planets at orbital periods shorter than 25 days. Solar-type stars with only giant planets with long orbital periods display mostly negative slopes, which may indicate that they do not host terrestrial planets, although there are some with positive slopes. The solar analogs without detected planets are more or less equally distributed above and below the flat slope.

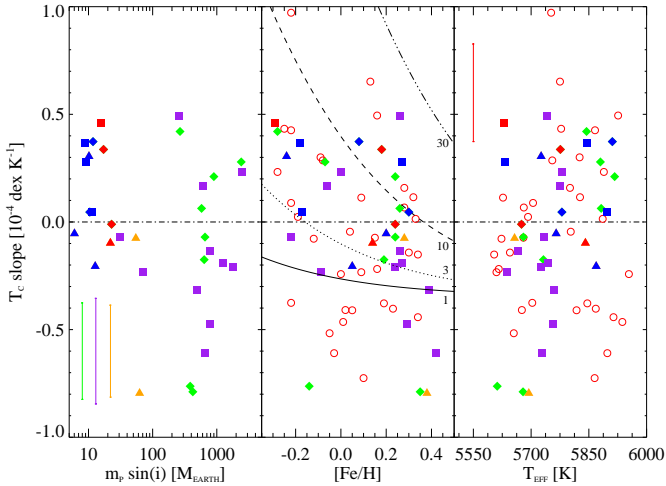


Fig. 12. Same as Fig. 11 but highlighting stars with super-Earth-like planets (red filled symbols) and stars with Neptune-like planets (blue filled symbols). The predicted lines (black lines) track the amount of rocky material in the planetary systems as 1, 3, 10, and $30 M_{\oplus}$.

Chambers (2010) demonstrates that it is possible to explain the abundances of solar twins in Meléndez et al. (2009) by adding four Earth masses of rocky material. In the solar system, the terrestrial planets only have about $2 M_{\oplus}$ of rock. However, the primordial asteroid belt probably contained a similar amount of rocky protoplanets (Weidenschilling 1977). This mass of rock was probably ejected from the solar system once Jupiter

formed (see e.g. Chambers & Wetherill 2001), and thus would be missed from the solar photosphere. Therefore, the existence of the present terrestrial planets and the asteroid belt in the solar planetary system could explain the abundance pattern of the solar twins with respect to the Sun. Chambers (2010) argues that just adding $4 M_{\oplus}$ of Earth-like material to the current solar photosphere is enough to sufficiently increase the amount of refractory elements but not to reproduce the abundance pattern of solar twins in Meléndez et al. (2009). To approximately recover that pattern one needs to add $4 M_{\oplus}$ of an equal mixture of Earth-like and CM chondrite material, provided that the fractionation is limited to the current size of the convection zone, which comprises $\sim 2.5\%$ of the Sun’s mass. Thus, this augmented solar abundance pattern roughly matches the mean abundance of those solar twins both for volatile and refractory elements, suggesting that the Sun could have accreted refractory-poor material from both the terrestrial-planet and the asteroid-belt regions (Chambers 2010).

One of the problems of this simple model is probably the size of the convection zone at the time of the formation of terrestrial planets. This issue has already been discussed in Meléndez et al. (2009) where they point out that protoplanetary disks have typical lifetimes $\lesssim 10$ Myr (see e.g. Sicilia-Aguilar et al. 2006; Mordasini et al. 2012), but at that time, the mass fraction of the convection zone of a solar-type star is about 40 % (D’Antona & Mazzitelli 1994), and it goes down to its current size likely after 30 Myr. However, recently Baraffe & Chabrier (2010) have shown that episodic accretion during pre-main-sequence evolution of solar-mass stars could accelerate the evolution of the convective zone until reaching its current size. This effect is more evident as the initial mass of the protostars, before the onset of the accretion episodes, decreases. Thus, only in the case of initial mass of the protostars before the onset of the accretion bursts as low as $10 M_{\text{Jup}}$ (with accretion rates of $0.5 M_{\text{Jup}} \text{ yr}^{-1}$ during episodes lasting for 100 yr) would the convection zone reach the current size in about 6–8 Myr, and therefore be consistent with the lifetime of the protoplanetary disk in the above scenario. Different efficiencies of episodic accretion may also affect the final atmospheric abundances of the star, as can the composition of the accreted material.

On the other hand, the accretion of small planets containing “heavy” refractory elements, which may happen, for instance, during inward migration of massive planets (as mentioned in section 6.5), may also affect the composition of the convective zone of these stars depending on the relative strength of thermohaline mixing/convection caused by unstable μ -gradient, external turbulence (as for instance rotation-induced mixing), and radiative levitation (see Vauclair & Théado 2012, and references therein). The remaining question may be how much this affects the accretion of volatiles elements such as C, N, and O, during accretion of the dust-depleted gas needed to explain the solar abundances in the above scenario.

Giant planets of the solar system also contain a significant number of refractory elements, $\sim 50 - 100 M_{\oplus}$ (Guillot 2005), but they do not appear to be enriched in rock-forming elements compared to ices (Owen et al. 1999). Thus, it is difficult to estimate how much giant-planet formation can affect the photospheric abundances of refractory elements in solar-type stars (see the discussion in Chambers 2010, for more details).

Chambers (2010) elaborates a simple model that quantifies the amount of rocky material in a stars’ planetary system from the slopes of the trends described by the abundance ratios of a sample of solar analogs versus the condensation temperature, T_c . They use the slopes derived by Ramírez et al. (2009) to

tentatively identify stars harboring terrestrial planets, according to their model. We applied this model to our sample of solar analogs, but we use the slopes determined with the average abundances in bins of $\Delta T_C = 150$ K as described in Section 6.6 and displayed in Fig. 11. We use both equations 1 and 2 in Chambers (2010) to estimate the mass of the accreted fractionated material, M_{frac} , which is mixed with material in the stellar convective zone, M_{CZ} , and the mass of rocky material, M_{rock} . We assume the mass of convective zone to be constant over time and equal to $0.02 M_{\odot}$ for all solar analogs (Pinsonneault et al. 2001). We also adopt the whole interval of condensation temperature 40–1750 K. We choose the value of -0.35×10^{-4} dex K^{-1} as minimum slope, which corresponds to the parameter S_{max} in Chambers (2010), since most of the points are above this value.

In Fig. 12, we depict the same plot as Fig. 11, but highlight those stars hosting super-Earth-like, with minimum masses, $m_p \sin i$, between 5 and $14 M_{\oplus}$, and Neptune-like, with $m_p \sin i$ 14– $30 M_{\oplus}$, planets. In the middle panel of Fig. 12 we also display lines corresponding to the amount of rocky material that is expected to be missed from the atmosphere of the stars according to their slopes. These lines should track the amount of mass that is in terrestrial planets, maybe also super-Earth-like planets, as well as possible asteroid belts. This plot is similar to Figure 3 in Chambers (2010), but the values used by Chambers (2010) are greater mainly because we subtract the chemical evolution effects from abundance trends of the stars, and Ramírez et al. (2009) did not. In addition, in this plot we distinguish among stars with and without known planets and with different minimum masses, which are super-Earth-like, Neptune-like, and giant planets. We note that we assume that at least super-Earth-like planets should contribute to the amount of missing rocky material from the stellar atmospheres. The position of the zero point depends on the adopted minimum slope, so we may only consider these lines as a tentative indication of the possible amount of terrestrial planets in the planetary systems of these solar analogs. This is probably a weak point of this simple model, which may only prevent us from drawing strong conclusions from this comparison. However, by using this value we are able to roughly reproduced the amount of rocky material in the solar planetary system, $M_{\text{rock}} \sim 4 M_{\oplus}$, which gives a flat slope at $[\text{Fe}/\text{H}] = 0$.

Figure 12 reveals that most of the stars may host certain amounts (more than $3 M_{\oplus}$) of terrestrial planets. In particular, between $3 M_{\oplus}$ and $10 M_{\oplus}$ there are many stars with already detected super-Earth-like planets, but there is no clear correlation between the slope values and amount of missing rocky material. Stars with known super-Earth-like planets with similar mass have in some cases very different predicted missing masses of rock. Thus, for instance, the star HD 45184 with only one super-Earth-like planet at $\sim 13 M_{\oplus}$ exhibits a negative slope but the predicted amount of rocky material is $\sim 2 M_{\oplus}$. The slope of the star HD 1461, which has two super-Earth-like planets accounting for a total mass of $\sim 14 M_{\oplus}$, yields a mass of rock of $\sim 6 M_{\oplus}$. The two stars with nearly flat slopes at about $+0.05 \times 10^{-4}$ dex K^{-1} , HD 31527 and HD 160691, and with low-mass planets at about $\sim 11 M_{\oplus}$, have however very different predicted rocky masses at ~ 3 and $\sim 10 M_{\oplus}$, respectively. This may mean that super-Earth-like planets are not traces of rocky missing material but only Earth-like planets are, or that the assumption that the slope of abundance trends versus condensation temperature are not related to the amount of terrestrial planets in the planetary systems of solar analogs.

In Fig. 12 we also depict stars with Neptune-like planets, which may also have rocky cores covered by volatile-rich at-

mospheres. Similarly we do not really know if super-Earth-like planets have an atmosphere or a crust rich in volatiles. Two stars with $\sim 17 M_{\oplus}$, have however significantly different predicted missing mass of rock from the stars' atmosphere at roughly $7 M_{\oplus}$ and $14 M_{\oplus}$. The size of the cores of these two planets are unknown, but if we assume that the cores are similar, then the star at higher metallicity may also harbor some undetected Earth-like planets. However, again we cannot prove this is the case but we also cannot demonstrate that the reasoning in Meléndez et al. (2009) and Ramírez et al. (2009) is correct.

6.8. Conclusions

We have explored the HARPS database to search for main-sequence stars with hotter effective temperature than the Sun and selected a sample in the T_{eff} range 5950–6400 K of 32 “single” stars and 29 stars hosting planets with high-resolution ($\lambda/\delta\lambda \gtrsim 85,000$) and very high signal-to-noise ($S/N \gtrsim 250$ and $S/N \sim 800$ on average) HARPS, UVES, and UES spectroscopic data. We tried to evaluate the possible connection between the abundance pattern versus the condensation temperature, T_C , and the presence of terrestrial planets.

We performed a detailed chemical abundance analysis of this sample of “hot” analogs and investigated possible trends of mean abundance ratios, $\Delta[\text{X}/\text{Fe}]_{\text{SUN-STARS}}$, versus T_C , after removing the Galactic chemical evolution effects. We find that stars both with and without planets show similar mean abundance patterns with slightly negative slopes. We also analyzed a subsample of metal-rich “hot” analogs in the narrow metallicity range $+0.04$ – $+0.19$ and also found negative slopes for stars both with and without planets, and almost equal mean abundance patterns when restricting the sample to very high quality spectra ($S/N > 550$).

We also revisited the sample of solar analogs in González Hernández et al. (2010) with the updated number of planet hosts, 62 “single” stars and 33 stars with planets. We investigated the mean abundance pattern of solar analogs harboring planets with the most massive planets at different orbital periods and with the least massive planet being a super-Earth-like, a Neptune-like, and a Jupiter-like planet. We speculated within the scenario in which the presence of rocky planets affect the volatile-to-refractory abundance ratios in the atmosphere of these planet-host stars. In each case the slope value reveals expected value according to this scenario, assuming that the bulk chemical composition of super-Earth planets is closer to the Earth's composition than that of Neptunian and Jovian planets.

This sample of solar analogs and of “hot” analogs have a subsample of eight and two stars harboring super-Earth-like planets. We computed the average abundance ratios $\Delta[\text{X}/\text{Fe}]_{\text{SUN-STARS}}$ versus condensation, T_C , in bins of $\Delta T_C = 150$ K, and individually fit these abundances to get the slope of the average abundance pattern of each star. We find that only four stars show positive abundance trends, qualitatively in agreement with the expected value according the reasoning in Meléndez et al. (2009) and Ramírez et al. (2009). However, three stars show nearly flat slopes, and three stars exhibit unexpected negative trends since they harbor super-Earth-like planets.

Finally, we derived the slopes of the trend $\Delta[\text{X}/\text{Fe}]_{\text{SUN-STARS}}$ versus T_C for each star of the whole sample of solar analogs and compared them with a simple model of the amount of rocky material missed in the stars' atmospheres. Several solar analogs containing super-Earth-like planets of typically $m_p \sin i \sim 11 M_{\oplus}$, with different slopes, provide very inconsis-

tent predictions of the missing amount of rocks from 2 to 15 M_{\oplus} . This might mean that only Earth-like planets could track the amount of missing rocky material in the atmospheres of solar analogs. Therefore, this comparison cannot provide clear evidence that in the abundance pattern of a solar-type star there are hints of terrestrial planets in the planetary system of each star.

Acknowledgements. J.I.G.H. and G.I. acknowledge financial support from the Spanish Ministry project MICINN AYA2011-29060 and J.I.G.H. also from the Spanish Ministry of Science and Innovation (MICINN) under the 2009 Juan de la Cierva Program. This work was also supported by the European Research Council/European Community under the FP7/EC through a Starting Grant agreement number 239953, as well as by Fundação para a Ciência e Tecnologia (FCT) in the form of grant reference PTDC/CTE-AST/098528/2008. N.C.S. would further like to thank FCT through program Ciência 2007 funded by FCT/MCTES (Portugal) and POPH/FSE (EC). V.Zh.A. and S.G.S. are supported by grants SFRH/BPD/70574/2010 and SFRH/BPD/47611/2008 from FCT (Portugal), respectively. E.D.M. is supported by grant SFRH/BPD/76606/2011 from FCT (Portugal). This research made use of the SIMBAD database operated at the CDS, Strasbourg, France. This work also made use of the IRAF facility and the Encyclopaedia of extrasolar planets.

References

- Adibekyan, V. Z., Delgado Mena, E., Sousa, S. G., et al. 2012a, *A&A*, 547, A36
 Adibekyan, V. Z., Santos, N. C., Sousa, S. G., et al. 2012b, *A&A*, 543, A89
 Adibekyan, V. Z., Sousa, S. G., Santos, N. C., et al. 2012c, *A&A*, 545, A32
 Allende Prieto, C., Lambert, D. L., & Asplund, M. 2001, *ApJ*, 556, L63
 Baraffe, I. & Chabrier, G. 2010, *A&A*, 521, A44
 Bensby, T., Feltzing, S., Lundström, I., & Ilyin, I. 2005, *A&A*, 433, 185
 Bond, J. C., O'Brien, D. P., & Laretta, D. S. 2010, *ApJ*, 715, 1050
 Buchhave, L. A., Latham, D. W., Johansen, A., et al. 2012, *Nature*, 486, 375
 Carter-Bond, J. C., O'Brien, D. P., Delgado Mena, E., et al. 2012a, *ApJ*, 747, L2
 Carter-Bond, J. C., O'Brien, D. P., & Raymond, S. N. 2012b, *ApJ*, 760, 44
 Chambers, J. E. 2010, *ApJ*, 724, 92
 Chambers, J. E. & Wetherill, G. W. 2001, *Meteoritics and Planetary Science*, 36, 381
 D'Antona, F. & Mazzitelli, I. 1994, *ApJS*, 90, 467
 Delgado Mena, E., Israelian, G., González Hernández, J. I., et al. 2010, *ApJ*, 725, 2349
 Ecuivillon, A., Israelian, G., Santos, N. C., Mayor, M., & Gilli, G. 2006, *A&A*, 449, 809
 Gilli, G., Israelian, G., Ecuivillon, A., Santos, N. C., & Mayor, M. 2006, *A&A*, 449, 723
 Gonzalez, G. 2011, *MNRAS*, 416, L80
 Gonzalez, G., Carlson, M. K., & Tobin, R. W. 2010, *MNRAS*, 407, 314
 González Hernández, J. I., Delgado-Mena, E., Sousa, S. G., et al. 2013a, in *AN*, Vol. 334, *Astron. Nachr.*, ed. —, —
 González Hernández, J. I., Delgado-Mena, E., Sousa, S. G., et al. 2013b, in *ASP Conference Series*, ed. —, *Astronomical Society of the Pacific*, —
 González Hernández, J. I., Israelian, G., Santos, N. C., et al. 2010, *ApJ*, 720, 1592
 González Hernández, J. I., Israelian, G., Santos, N. C., et al. 2011a, in *Highlights of Spanish Astrophysics VI*, ed. M. R. Zapatero Osorio, J. Gorgas, J. Maíz Apellániz, J. R. Pardo, & A. Gil de Paz, 576–582
 González Hernández, J. I., Israelian, G., Santos, N. C., et al. 2011b, in *IAU Symposium*, Vol. 276, *IAU Symposium*, ed. A. Sozzetti, M. G. Lattanzi, & A. P. Boss, 422–423
 Guillot, T. 2005, *Annual Review of Earth and Planetary Sciences*, 33, 493
 Howard, A. W., Marcy, G. W., Johnson, J. A., et al. 2010, *Science*, 330, 653
 Jorissen, A., Mayor, M., & Udry, S. 2001, *A&A*, 379, 992
 Kargel, J. S. & Lewis, J. S. 1993, *Icarus*, 105, 1
 Kurucz, R. 1993, *ATLAS9 Stellar Atmosphere Programs and 2 km/s grid*. Kurucz CD-ROM No. 13. Cambridge, Mass.: Smithsonian Astrophysical Observatory, 1993., 13
 Kurucz, R. L., Furenlid, I., Brault, J., & Testerman, L. 1984, *Solar flux atlas from 296 to 1300 nm*
 Lambert, D. L. 1978, *MNRAS*, 182, 249
 Laws, C. & Gonzalez, G. 2001, *ApJ*, 553, 405
 Lodders, K. 2003, *ApJ*, 591, 1220
 Lovis, C., Ségransan, D., Mayor, M., et al. 2011, *A&A*, 528, A112
 Marcy, G., Butler, R. P., Fischer, D., et al. 2005, *Progress of Theoretical Physics Supplement*, 158, 24
 Mayor, M., Marmier, M., Lovis, C., et al. 2011, *ArXiv e-prints*
 Mayor, M., Pepe, F., Queloz, D., et al. 2003, *The Messenger*, 114, 20
 Mayor, M. & Udry, S. 2008, *Physica Scripta Volume T*, 130, 014010
 Mayor, M., Udry, S., Lovis, C., et al. 2009, *A&A*, 493, 639
 Meléndez, J., Asplund, M., Gustafsson, B., & Yong, D. 2009, *ApJ*, 704, L66
 Meléndez, J., Bergemann, M., Cohen, J. G., et al. 2012, *A&A*, 543, A29
 Mordasini, C., Alibert, Y., & Benz, W. 2009a, *A&A*, 501, 1139
 Mordasini, C., Alibert, Y., Benz, W., Klahr, H., & Henning, T. 2012, *A&A*, 541, A97
 Mordasini, C., Alibert, Y., Benz, W., & Naef, D. 2009b, *A&A*, 501, 1161
 Neves, V., Santos, N. C., Sousa, S. G., Correia, A. C. M., & Israelian, G. 2009, *A&A*, 497, 563
 Owen, T., Mahaffy, P., Niemann, H. B., et al. 1999, *Nature*, 402, 269
 Pinsonneault, M. H., DePoy, D. L., & Coffee, M. 2001, *ApJ*, 556, L59
 Ramírez, I., Asplund, M., Baumann, P., Meléndez, J., & Bensby, T. 2010, *A&A*, 521, A33
 Ramírez, I., Meléndez, J., & Asplund, M. 2009, *A&A*, 508, L17
 Ramírez, I., Meléndez, J., Cornejo, D., Roederer, I. U., & Fish, J. R. 2011, *ApJ*, 740, 76
 Reddy, B. E., Lambert, D. L., & Allende Prieto, C. 2006, *MNRAS*, 367, 1329
 Santos, N. C., Israelian, G., & Mayor, M. 2001, *A&A*, 373, 1019
 Santos, N. C., Israelian, G., & Mayor, M. 2004, *A&A*, 415, 1153
 Schuler, S. C., Cunha, K., Smith, V. V., et al. 2011a, *ApJ*, 737, L32
 Schuler, S. C., Flateau, D., Cunha, K., et al. 2011b, *ApJ*, 732, 55
 Sicilia-Aguilar, A., Hartmann, L., Calvet, N., et al. 2006, *ApJ*, 638, 897
 Sneden, C. A. 1973, PhD thesis, THE UNIVERSITY OF TEXAS AT AUSTIN.
 Sousa, S. G., Santos, N. C., Israelian, G., Mayor, M., & Monteiro, M. J. P. F. G. 2007, *A&A*, 469, 783
 Sousa, S. G., Santos, N. C., Israelian, G., Mayor, M., & Udry, S. 2011, *A&A*, 533, A141
 Sousa, S. G., Santos, N. C., Mayor, M., et al. 2008, *A&A*, 487, 373
 Takeda, Y. 2005, *PASJ*, 57, 83
 Takeda, Y. 2007, *PASJ*, 59, 335
 Udry, S., Mayor, M., Benz, W., et al. 2006, *A&A*, 447, 361
 Udry, S. & Santos, N. C. 2007, *ARA&A*, 45, 397
 Valencia, D., O'Connell, R. J., & Sasselov, D. D. 2007a, *ApJ*, 670, L45
 Valencia, D., Sasselov, D. D., & O'Connell, R. J. 2007b, *ApJ*, 665, 1413
 Valenti, J. A. & Fischer, D. A. 2005, *ApJS*, 159, 141
 Vauclair, S. & Théado, S. 2012, *ApJ*, 753, 49
 Weidenschilling, S. J. 1977, *Ap&SS*, 51, 153

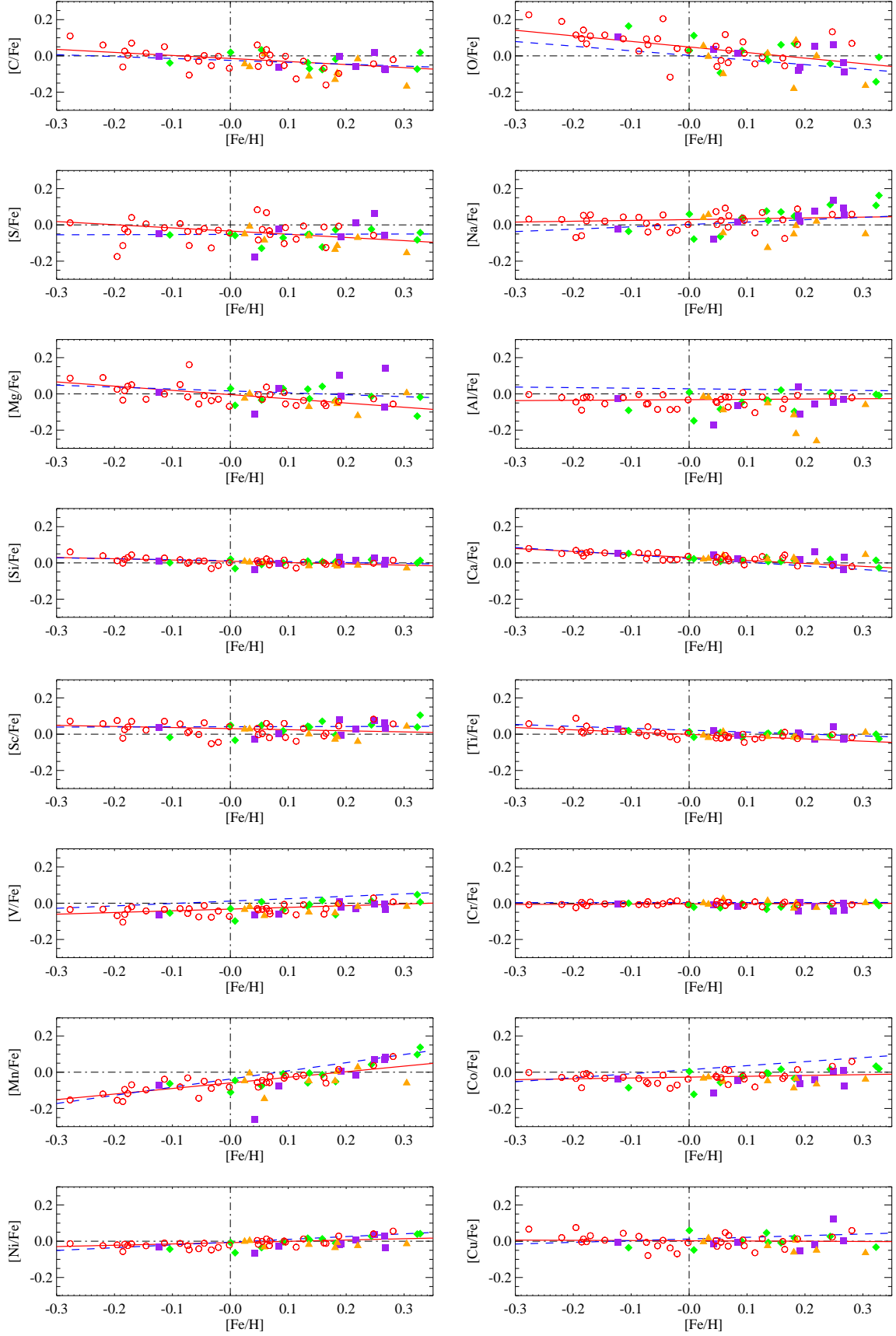


Fig. 2. Chemical abundance ratios $[X/Fe]$ versus $[Fe/H]$ for the whole sample of “hot” analogs, containing 32 “single” stars (red open circles) and 29 stars hosting planets, with the most massive planet in an orbital period $P_{\text{orb}} < 65$ days (green filled diamonds), $115 < P_{\text{orb}} < 630$ days (violet filled squares), $950 < P_{\text{orb}} < 4050$ days (orange filled triangles). Red solid lines provide linear fits to the data points of the 32 “single” stars, whereas blue dashed lines show the linear fits to the data points of “single” solar analogs in González Hernández et al. (2010).

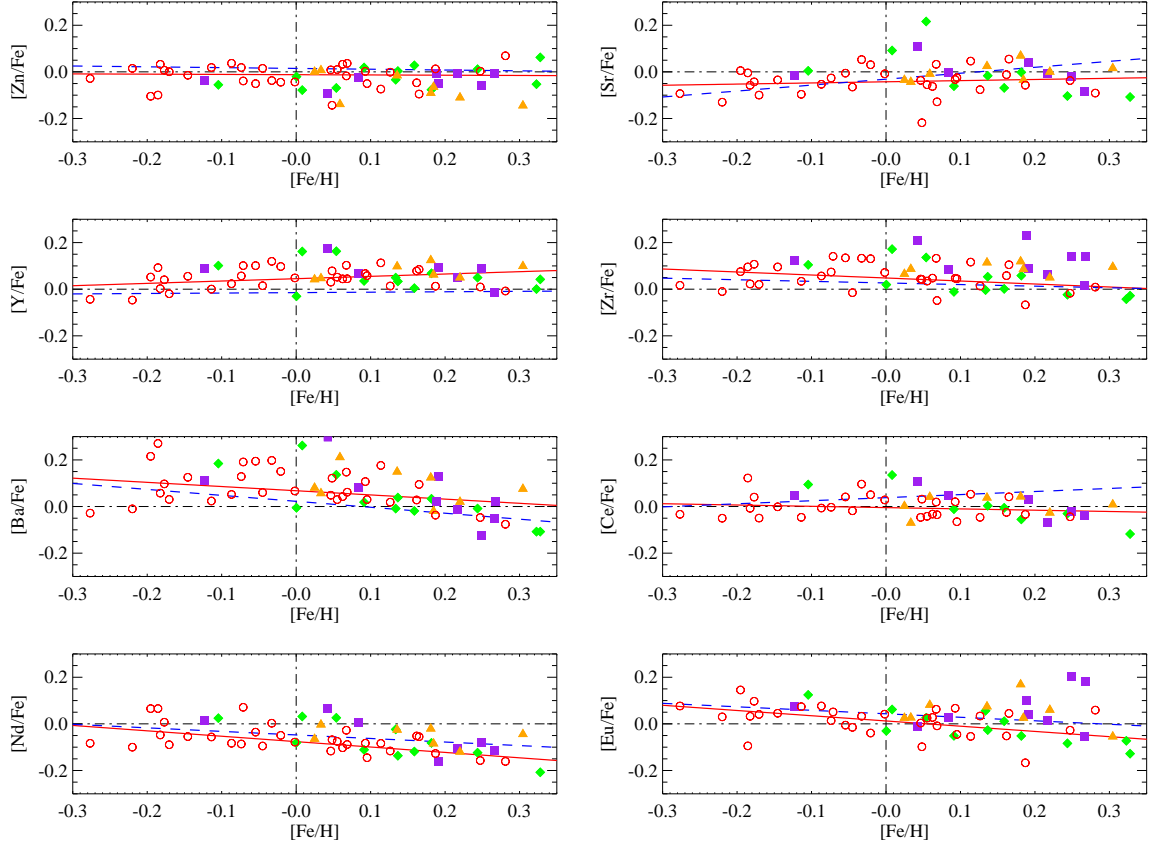


Fig. 3. Fig. 2 continued.

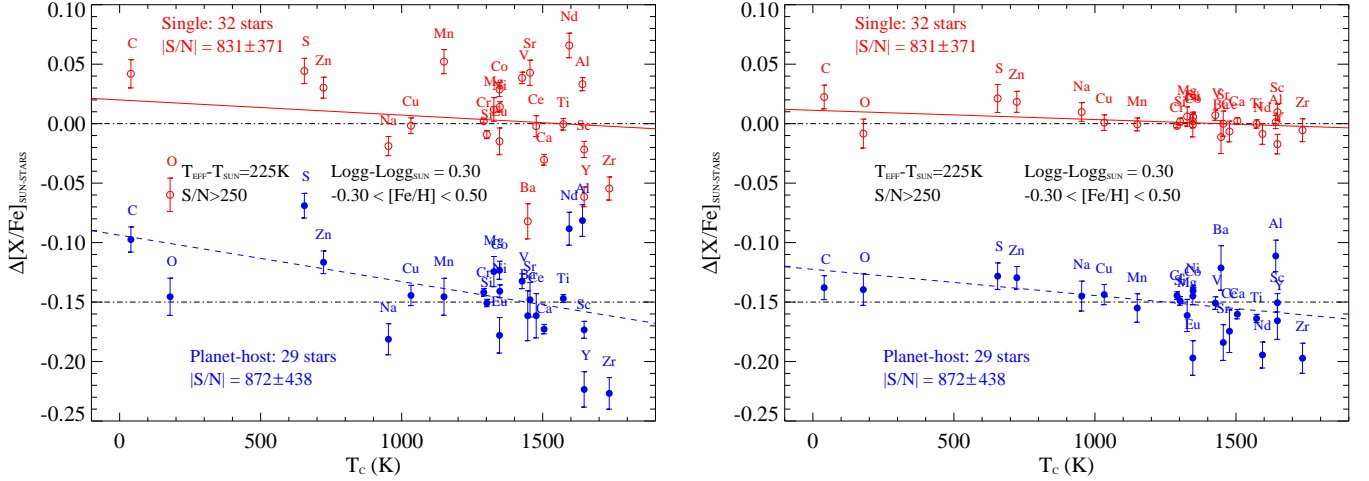


Fig. 4. Mean abundance differences, $\Delta[X/Fe]_{\text{SUN-STARS}}$, between the Sun, 29 planet hosts (blue filled circles), and 32 “single” stars (red open circles) of the sample of all “hot” analogs. Error bars are the standard deviation from the mean divided by the square root of the number of stars. The points of stars hosting planets have been artificially shifted by -0.15 dex for the sake of clarity. Linear fits to the data points weighted with the error bars are also displayed for planet hosts (dashed line) and “single” stars (red solid line). The right panel shows the results after removing the galactic chemical evolution effects using the linear fits to the 32 “single” stars.

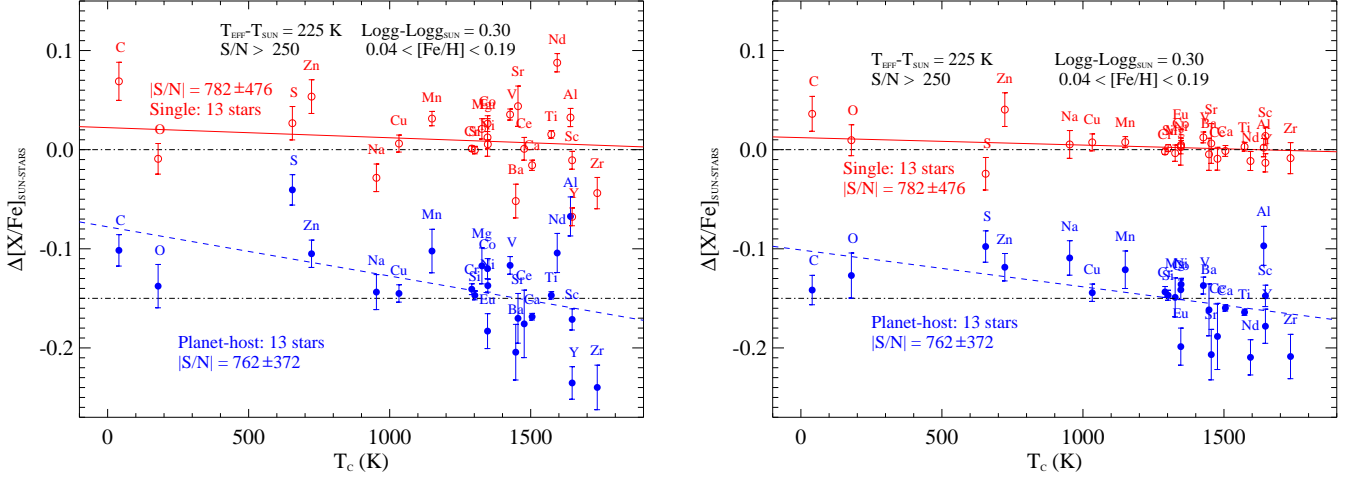


Fig. 5. Same as in Fig. 4 for 13 planet hosts and 13 “single” stars of the sample of metal-rich “hot” analogs.

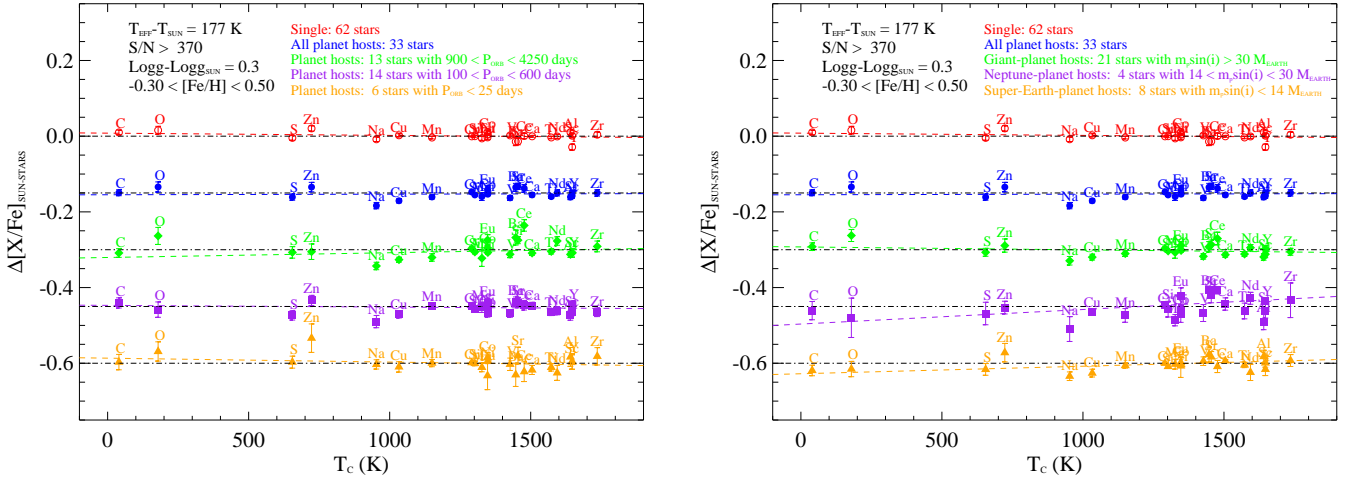


Fig. 6. *Left panel:* Same as right panel in Fig. 4 but for solar analogs containing 62 “single” stars (red open circles) and 33 stars hosting planets (blue filled circles), with the most massive planet in an orbital period $P_{\text{orb}} < 25$ days (6 stars, yellow filled triangles), $100 < P_{\text{orb}} < 600$ days (14 stars, violet filled squares), $900 < P_{\text{orb}} < 4250$ days (13 stars, green filled triangles). The mean abundance differences, $\Delta[X/H]_{\text{SUN-STARS}}$, and linear fits have been artificially shifted by -0.15 dex, for the sake of clarity. Horizontal dashed-dot lines show the zero point levels for each set of points. *Right panel:* Same as left panel but for planet-host stars with the minimum mass of the least massive planet in the ranges: $m_p \sin i < 14 M_{\oplus}$ (8 stars, yellow filled triangles), $14 < m_p \sin i < 30 M_{\oplus}$ (4 stars, violet filled squares), $m_p \sin i > 30 M_{\oplus}$ (21 stars, green filled triangles).

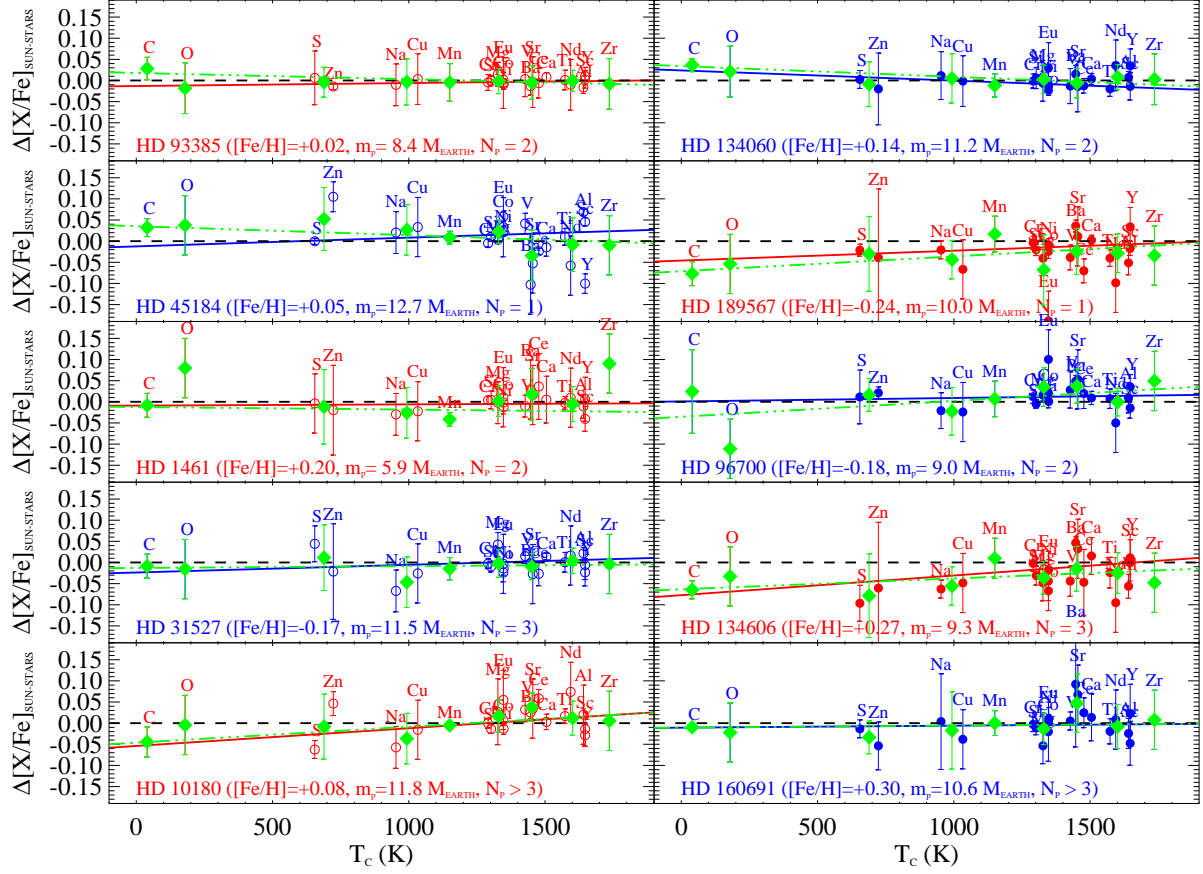


Fig. 7. Abundance differences, $\Delta[X/Fe]_{\text{SUN-STARS}}$, between the Sun and 10 stars hosting super-Earth-like planets (circles), 2 corresponding to the sample of “hot” analogs (top panels) and 8 belong to the sample of solar analogs analyzed in González Hernández et al. (2010). Error bars are the uncertainties of the element abundance measurements, corresponding to the line-by-line scatter. Diamonds show the average abundances in bins of $\Delta T_c = 150$ K. Error bars are the standard deviation from the mean abundance of the elements in each T_c bin. Linear fits to the data points (solid line) and to the mean data points (dashed-dotted line) weighted with the error bars are also displayed.

Appendix A: Chemical abundance ratios [X/Fe]

In this appendix we provide all the tables containing the element abundance ratios [X/Fe] of 32 F-, G-type stars without planets and 29 F-, G-type stars hosting planets that are all available on-line.

Table A.1. Abundance ratios [X/Fe] of F-, G-type analogs with planets

HD	[C/Fe]	[O/Fe]	[S/Fe]	[Na/Fe]	[Mg/Fe]	[Al/Fe]
10647	–	0.112 ± 0.070	–0.058 ± 0.042	–0.078 ± 0.057	–0.063 ± 0.064	–0.148 ± 0.014
108147	–0.131 ± 0.028	–0.181 ± 0.070	–0.136 ± 0.007	–0.051 ± 0.057	–0.041 ± 0.057	–0.116 ± 0.007
117618	–0.060 ± 0.049	–0.003 ± 0.070	–0.008 ± 0.049	0.057 ± 0.042	0.002 ± 0.021	–0.018 ± 0.021
121504	–0.112 ± 0.042	0.014 ± 0.070	–0.061 ± 0.120	–0.126 ± 0.085	–0.071 ± 0.049	–0.051 ± 0.035
134060	–0.070 ± 0.015	–0.027 ± 0.070	–0.052 ± 0.021	0.023 ± 0.057	–0.027 ± 0.042	–0.037 ± 0.014
169830	–0.018 ± 0.068	0.068 ± 0.070	–0.027 ± 0.092	0.048 ± 0.057	–0.037 ± 0.021	–0.097 ± 0.021
17051	–	–0.061 ± 0.070	–0.066 ± 0.007	0.019 ± 0.070	–0.011 ± 0.113	–0.111 ± 0.070
179949	–0.017 ± 0.127	0.000 ± 0.070	–0.070 ± 0.028	0.020 ± 0.014	–0.120 ± 0.028	–0.260 ± 0.028
19994	0.018 ± 0.068	0.061 ± 0.070	0.061 ± 0.070	0.136 ± 0.021	–	–0.049 ± 0.070
208487	–0.064 ± 0.030	0.016 ± 0.070	–0.024 ± 0.070	0.016 ± 0.042	0.031 ± 0.106	–0.064 ± 0.028
212301	–0.094 ± 0.028	0.086 ± 0.070	–0.114 ± 0.057	–0.004 ± 0.071	–0.054 ± 0.057	–0.219 ± 0.021
216435	–	–0.044 ± 0.070	–0.024 ± 0.070	0.111 ± 0.021	–0.014 ± 0.014	0.006 ± 0.042
221287	–	0.037 ± 0.070	–0.178 ± 0.021	–0.078 ± 0.021	–0.113 ± 0.014	–0.173 ± 0.070
23079	–0.001 ± 0.045	0.103 ± 0.070	–0.047 ± 0.042	–0.022 ± 0.064	0.008 ± 0.021	–0.027 ± 0.028
39091	–	0.029 ± 0.070	–0.071 ± 0.028	0.039 ± 0.057	0.029 ± 0.042	–0.046 ± 0.035
7449	–0.039 ± 0.035	0.164 ± 0.070	–0.055 ± 0.042	–0.035 ± 0.057	–	–0.090 ± 0.007
75289	–0.168 ± 0.025	–0.165 ± 0.070	–0.155 ± 0.127	–0.050 ± 0.035	0.005 ± 0.042	–0.060 ± 0.007
82943	–0.069 ± 0.021	–0.036 ± 0.070	–0.056 ± 0.085	0.094 ± 0.070	–0.071 ± 0.120	–0.031 ± 0.021
93385	–0.045 ± 0.026	0.055 ± 0.070	–0.050 ± 0.064	0.040 ± 0.049	–0.025 ± 0.028	–0.015 ± 0.014
209458	0.011 ± 0.070	–0.099 ± 0.070	–0.084 ± 0.064	–0.044 ± 0.064	–	–0.089 ± 0.014
2039	–0.073 ± 0.106	–0.143 ± 0.070	–0.083 ± 0.042	0.107 ± 0.028	–0.123 ± 0.070	–0.003 ± 0.028
213240	–0.075 ± 0.025	0.061 ± 0.070	–0.122 ± 0.029	0.071 ± 0.042	0.041 ± 0.042	0.021 ± 0.028
23596	0.019 ± 0.076	–0.008 ± 0.070	–0.043 ± 0.035	0.162 ± 0.071	–0.018 ± 0.014	–0.008 ± 0.014
50554	0.033 ± 0.101	–0.094 ± 0.070	–0.129 ± 0.035	–0.064 ± 0.042	–0.034 ± 0.042	–0.084 ± 0.014
52265	–0.060 ± 0.047	0.053 ± 0.070	0.013 ± 0.057	0.078 ± 0.035	–	–0.057 ± 0.028
72659	0.020 ± 0.040	0.030 ± 0.070	–0.050 ± 0.085	0.060 ± 0.042	0.030 ± 0.070	0.010 ± 0.014
74156	–0.037 ± 0.025	0.006 ± 0.070	–0.054 ± 0.071	0.076 ± 0.057	0.026 ± 0.070	–0.034 ± 0.014
89744	–0.078 ± 0.014	–0.088 ± 0.070	–	0.052 ± 0.042	0.142 ± 0.070	–
9826	–0.003 ± 0.007	–0.078 ± 0.070	–	0.052 ± 0.042	0.102 ± 0.070	0.037 ± 0.148

Table A.2. Abundance ratios [X/Fe] of F-, G-type analogs with planets

HD	[Si/Fe]	[Ca/Fe]	[Sc/Fe]	[Ti/Fe]	[V/Fe]	[Cr/Fe]
10647	-0.031 ± 0.016	0.023 ± 0.024	-0.033 ± 0.031	-0.016 ± 0.031	-0.098 ± 0.049	-0.022 ± 0.040
108147	-0.010 ± 0.019	0.028 ± 0.021	-0.028 ± 0.010	-0.016 ± 0.033	-0.054 ± 0.041	-0.029 ± 0.025
117618	0.004 ± 0.018	0.024 ± 0.032	0.029 ± 0.030	-0.019 ± 0.016	-0.018 ± 0.006	-0.006 ± 0.017
121504	-0.016 ± 0.015	0.021 ± 0.024	0.000 ± 0.034	-0.014 ± 0.017	-0.050 ± 0.015	0.014 ± 0.007
134060	-0.006 ± 0.025	0.008 ± 0.013	0.039 ± 0.032	0.005 ± 0.017	-0.007 ± 0.041	-0.002 ± 0.017
169830	0.007 ± 0.016	0.014 ± 0.048	-0.004 ± 0.027	-0.014 ± 0.034	-0.064 ± 0.030	-0.021 ± 0.023
17051	-0.006 ± 0.029	0.017 ± 0.031	-0.004 ± 0.074	-0.003 ± 0.050	-0.021 ± 0.084	0.002 ± 0.019
179949	-0.013 ± 0.040	0.005 ± 0.033	-0.040 ± 0.010	-0.022 ± 0.037	-0.018 ± 0.058	-0.025 ± 0.026
19994	0.027 ± 0.032	-0.007 ± 0.029	0.076 ± 0.019	0.041 ± 0.044	-0.005 ± 0.075	-0.042 ± 0.056
208487	-0.004 ± 0.009	0.021 ± 0.010	0.004 ± 0.022	-0.004 ± 0.024	-0.062 ± 0.040	-0.018 ± 0.019
212301	-0.019 ± 0.034	0.014 ± 0.016	-0.014 ± 0.048	-0.016 ± 0.034	-0.006 ± 0.041	0.001 ± 0.021
216435	0.018 ± 0.015	0.019 ± 0.029	0.051 ± 0.025	-0.008 ± 0.035	0.012 ± 0.044	-0.018 ± 0.027
221287	-0.035 ± 0.014	0.044 ± 0.032	-0.028 ± 0.017	0.020 ± 0.034	-0.066 ± 0.088	-0.009 ± 0.043
23079	0.008 ± 0.007	0.051 ± 0.010	0.037 ± 0.036	0.029 ± 0.021	-0.064 ± 0.040	-0.002 ± 0.020
39091	0.001 ± 0.013	0.013 ± 0.017	0.019 ± 0.042	-0.018 ± 0.026	-0.038 ± 0.025	-0.002 ± 0.013
7449	0.001 ± 0.007	0.052 ± 0.018	-0.017 ± 0.026	0.020 ± 0.025	-0.054 ± 0.045	-0.000 ± 0.026
75289	-0.028 ± 0.028	0.045 ± 0.030	0.043 ± 0.054	0.010 ± 0.024	-0.018 ± 0.045	0.002 ± 0.014
82943	-0.006 ± 0.018	-0.036 ± 0.062	0.064 ± 0.037	-0.027 ± 0.026	-0.004 ± 0.023	0.000 ± 0.017
93385	0.008 ± 0.013	0.020 ± 0.010	0.028 ± 0.021	-0.006 ± 0.023	-0.035 ± 0.042	0.001 ± 0.019
209458	0.002 ± 0.056	0.041 ± 0.055	-	0.014 ± 0.090	-0.069 ± 0.029	0.024 ± 0.133
2039	-0.000 ± 0.017	0.014 ± 0.036	0.039 ± 0.047	-0.000 ± 0.029	0.047 ± 0.007	0.006 ± 0.012
213240	0.007 ± 0.012	0.008 ± 0.032	0.071 ± 0.055	0.008 ± 0.023	0.015 ± 0.025	-0.022 ± 0.016
23596	0.014 ± 0.039	-0.027 ± 0.045	0.105 ± 0.022	-0.025 ± 0.034	0.006 ± 0.023	-0.013 ± 0.039
50554	-0.009 ± 0.049	0.009 ± 0.034	0.049 ± 0.006	0.009 ± 0.049	0.008 ± 0.058	-0.025 ± 0.044
52265	0.015 ± 0.020	0.061 ± 0.033	0.028 ± 0.033	-0.027 ± 0.021	-0.031 ± 0.023	-0.015 ± 0.033
72659	0.021 ± 0.012	0.026 ± 0.014	0.050 ± 0.026	0.014 ± 0.015	-0.030 ± 0.038	-0.008 ± 0.008
74156	0.010 ± 0.010	0.030 ± 0.038	0.044 ± 0.010	0.000 ± 0.029	-0.017 ± 0.027	-0.034 ± 0.019
89744	0.015 ± 0.034	0.030 ± 0.034	0.035 ± 0.043	-0.021 ± 0.052	-0.036 ± 0.067	-0.038 ± 0.028
9826	0.032 ± 0.031	0.017 ± 0.014	0.080 ± 0.024	0.009 ± 0.058	0.010 ± 0.077	-0.043 ± 0.044

Table A.3. Abundance ratios [X/Fe] of F-, G-type analogs with planets

HD	[Mn/Fe]	[Co/Fe]	[Ni/Fe]	[Cu/Fe]	[Zn/Fe]	[Sr/Fe]
10647	-0.046 ± 0.083	-0.122 ± 0.037	-0.064 ± 0.024	-0.048 ± 0.070	-0.078 ± 0.028	0.092 ± 0.070
108147	-0.048 ± 0.033	-0.088 ± 0.024	-0.036 ± 0.030	-0.061 ± 0.070	-0.091 ± 0.042	0.069 ± 0.070
117618	-0.006 ± 0.026	-0.027 ± 0.009	0.003 ± 0.015	0.017 ± 0.070	0.007 ± 0.014	-0.043 ± 0.070
121504	-0.048 ± 0.021	-0.049 ± 0.005	-0.018 ± 0.016	-0.026 ± 0.070	-0.016 ± 0.057	0.024 ± 0.070
134060	-0.005 ± 0.028	-0.007 ± 0.006	0.008 ± 0.022	-0.007 ± 0.070	0.003 ± 0.085	-0.017 ± 0.070
169830	-0.052 ± 0.054	-0.035 ± 0.024	-0.011 ± 0.023	0.018 ± 0.070	-0.077 ± 0.021	-0.002 ± 0.070
17051	0.006 ± 0.046	-0.063 ± 0.027	-0.013 ± 0.027	-0.051 ± 0.070	-0.051 ± 0.028	0.039 ± 0.070
179949	0.028 ± 0.021	-0.066 ± 0.029	-0.025 ± 0.028	-0.050 ± 0.070	-0.110 ± 0.042	0.000 ± 0.070
19994	0.069 ± 0.017	0.006 ± 0.051	0.037 ± 0.028	0.121 ± 0.070	-0.059 ± 0.070	-0.019 ± 0.070
208487	-0.074 ± 0.067	-0.046 ± 0.029	-0.025 ± 0.019	-0.004 ± 0.070	-0.024 ± 0.057	-0.004 ± 0.070
212301	0.003 ± 0.094	-0.036 ± 0.056	-0.009 ± 0.030	0.006 ± 0.070	-0.064 ± 0.042	-0.034 ± 0.070
216435	0.042 ± 0.073	0.016 ± 0.015	0.028 ± 0.026	0.026 ± 0.070	0.011 ± 0.120	-0.104 ± 0.070
221287	-0.260 ± 0.103	-0.116 ± 0.034	-0.068 ± 0.032	-0.013 ± 0.070	-0.093 ± 0.070	0.107 ± 0.070
23079	-0.070 ± 0.070	-0.039 ± 0.024	-0.031 ± 0.014	-0.007 ± 0.070	-0.037 ± 0.014	-0.017 ± 0.070
39091	-0.009 ± 0.031	-0.025 ± 0.005	-0.003 ± 0.010	-0.001 ± 0.070	0.019 ± 0.042	-0.061 ± 0.070
7449	-0.063 ± 0.079	-0.085 ± 0.017	-0.044 ± 0.012	-0.035 ± 0.070	-0.055 ± 0.014	0.005 ± 0.070
75289	-0.060 ± 0.057	-0.039 ± 0.022	-0.015 ± 0.026	-0.065 ± 0.070	-0.145 ± 0.057	0.015 ± 0.070
82943	0.072 ± 0.019	0.010 ± 0.025	0.029 ± 0.019	0.004 ± 0.070	-0.006 ± 0.042	-0.086 ± 0.070
93385	-0.049 ± 0.045	-0.033 ± 0.017	-0.002 ± 0.012	-0.005 ± 0.070	0.000 ± 0.007	-0.035 ± 0.070
209458	-0.146 ± 0.062	-0.051 ± 0.133	-0.032 ± 0.110	–	-0.139 ± 0.070	-0.009 ± 0.070
2039	0.097 ± 0.070	0.033 ± 0.023	0.039 ± 0.038	-0.033 ± 0.070	-0.053 ± 0.070	–
213240	-0.014 ± 0.029	0.016 ± 0.012	0.013 ± 0.020	-0.009 ± 0.070	0.028 ± 0.040	-0.069 ± 0.070
23596	0.137 ± 0.031	0.019 ± 0.030	0.042 ± 0.029	–	0.062 ± 0.113	-0.108 ± 0.070
50554	-0.076 ± 0.102	-0.057 ± 0.025	-0.035 ± 0.037	–	-0.069 ± 0.134	0.216 ± 0.070
52265	-0.015 ± 0.067	-0.040 ± 0.031	0.006 ± 0.026	-0.017 ± 0.070	-0.007 ± 0.017	-0.007 ± 0.070
72659	-0.110 ± 0.071	0.005 ± 0.005	-0.007 ± 0.020	0.060 ± 0.070	-0.020 ± 0.070	–
74156	-0.059 ± 0.092	-0.004 ± 0.012	0.016 ± 0.028	0.046 ± 0.070	-0.034 ± 0.070	–
89744	0.082 ± 0.099	-0.074 ± 0.047	-0.038 ± 0.044	–	–	–
9826	–	-0.031 ± 0.032	-0.017 ± 0.039	–	-0.008 ± 0.070	–

Table A.4. Abundance ratios [X/Fe] of F-, G-type analogs with planets

HD	[Y/Fe]	[Zr/Fe]	[Ba/Fe]	[Ce/Fe]	[Nd/Fe]	[Eu/Fe]
10647	0.162 ± 0.026	0.172 ± 0.070	0.262 ± 0.042	0.135 ± 0.074	0.032 ± 0.070	0.062 ± 0.070
108147	0.124 ± 0.049	0.119 ± 0.070	0.124 ± 0.064	0.042 ± 0.006	-0.021 ± 0.070	0.169 ± 0.070
117618	0.047 ± 0.020	0.087 ± 0.070	0.057 ± 0.070	-0.070 ± 0.031	-0.003 ± 0.070	0.027 ± 0.070
121504	0.098 ± 0.035	0.114 ± 0.070	0.149 ± 0.021	0.038 ± 0.015	-0.026 ± 0.070	0.074 ± 0.070
134060	0.033 ± 0.040	0.053 ± 0.070	0.038 ± 0.021	0.003 ± 0.017	-0.137 ± 0.070	-0.027 ± 0.070
169830	0.068 ± 0.044	0.058 ± 0.070	0.033 ± 0.021	-0.055 ± 0.067	-0.082 ± 0.070	-0.052 ± 0.070
17051	0.092 ± 0.055	0.089 ± 0.070	0.128 ± 0.099	0.029 ± 0.026	-0.161 ± 0.070	0.039 ± 0.070
179949	0.050 ± 0.028	0.050 ± 0.070	0.020 ± 0.028	-0.027 ± 0.012	-0.120 ± 0.070	0.060 ± 0.070
19994	0.088 ± 0.090	0.141 ± 0.070	-0.124 ± 0.007	-0.022 ± 0.057	-0.079 ± 0.070	0.201 ± 0.070
208487	0.069 ± 0.050	0.086 ± 0.070	0.081 ± 0.021	0.049 ± 0.021	0.006 ± 0.070	0.026 ± 0.070
212301	0.062 ± 0.025	0.086 ± 0.070	-0.019 ± 0.021	-	-0.084 ± 0.070	0.025 ± 0.070
216435	0.050 ± 0.059	-0.024 ± 0.070	-0.009 ± 0.021	-0.030 ± 0.035	-0.124 ± 0.070	-0.084 ± 0.070
221287	0.174 ± 0.021	0.207 ± 0.070	0.297 ± 0.085	0.107 ± 0.123	0.067 ± 0.070	-0.013 ± 0.070
23079	0.089 ± 0.029	0.123 ± 0.070	0.113 ± 0.070	0.049 ± 0.051	0.013 ± 0.070	0.073 ± 0.070
39091	0.035 ± 0.031	-0.011 ± 0.070	0.019 ± 0.070	-0.011 ± 0.036	-0.111 ± 0.070	-0.051 ± 0.070
7449	0.101 ± 0.029	0.105 ± 0.070	0.185 ± 0.070	0.095 ± 0.052	0.025 ± 0.070	0.125 ± 0.070
75289	0.099 ± 0.042	0.095 ± 0.070	0.075 ± 0.070	0.009 ± 0.023	-0.045 ± 0.070	-0.055 ± 0.070
82943	-0.016 ± 0.040	0.014 ± 0.070	-0.051 ± 0.049	-0.039 ± 0.064	-0.116 ± 0.070	-0.056 ± 0.070
93385	0.042 ± 0.021	0.065 ± 0.070	0.080 ± 0.021	0.002 ± 0.035	-0.065 ± 0.070	0.025 ± 0.070
209458	-	-	0.211 ± 0.085	0.041 ± 0.072	-	0.081 ± 0.070
2039	0.001 ± 0.015	-0.043 ± 0.070	-0.108 ± 0.021	-	-	-0.073 ± 0.070
213240	0.005 ± 0.042	0.001 ± 0.070	-0.019 ± 0.028	-0.005 ± 0.006	-0.119 ± 0.070	0.011 ± 0.070
23596	0.042 ± 0.035	-0.028 ± 0.070	-0.108 ± 0.070	-0.118 ± 0.141	-0.208 ± 0.070	-0.128 ± 0.070
50554	0.163 ± 0.045	0.136 ± 0.070	0.136 ± 0.085	0.321 ± 0.092	0.026 ± 0.070	0.026 ± 0.070
52265	0.050 ± 0.047	0.063 ± 0.070	-0.012 ± 0.007	-0.071 ± 0.025	-0.107 ± 0.070	0.013 ± 0.070
72659	-0.030 ± 0.044	0.020 ± 0.070	-0.005 ± 0.007	-	-0.080 ± 0.070	-0.030 ± 0.070
74156	0.050 ± 0.058	-0.004 ± 0.070	-0.009 ± 0.021	-	-0.024 ± 0.070	0.056 ± 0.070
89744	-	0.142 ± 0.070	0.022 ± 0.070	-	-	0.182 ± 0.070
9826	-	0.232 ± 0.070	0.022 ± 0.028	-	-	0.102 ± 0.070

Table A.5. Abundance ratios [X/Fe] of F-, G-type analogs without known planets

HD	[C/Fe]	[O/Fe]	[S/Fe]	[Na/Fe]	[Mg/Fe]	[Al/Fe]
11226	0.060 ± 0.042	0.054 ± 0.070	0.083 ± 0.070	0.073 ± 0.042	–	–0.042 ± 0.021
119638	0.016 ± 0.044	0.116 ± 0.070	0.006 ± 0.057	0.021 ± 0.064	–0.029 ± 0.035	–0.054 ± 0.028
122862	0.050 ± 0.035	0.094 ± 0.070	–0.016 ± 0.042	0.044 ± 0.042	–0.001 ± 0.021	–0.021 ± 0.035
125881	–0.037 ± 0.070	–0.037 ± 0.070	–0.032 ± 0.049	–0.012 ± 0.035	–	–0.072 ± 0.021
1388	–0.068 ± 0.020	0.032 ± 0.070	–0.043 ± 0.078	0.002 ± 0.042	–0.068 ± 0.099	–0.033 ± 0.007
145666	–0.054 ± 0.071	–0.117 ± 0.070	–0.127 ± 0.070	–0.042 ± 0.035	–0.037 ± 0.014	–0.087 ± 0.028
157338	–0.011 ± 0.035	0.094 ± 0.070	–0.036 ± 0.028	0.009 ± 0.064	–0.016 ± 0.070	–0.056 ± 0.028
1581	0.004 ± 0.060	0.067 ± 0.070	–0.038 ± 0.007	0.022 ± 0.049	0.042 ± 0.035	–0.018 ± 0.035
168871	–	0.027 ± 0.070	0.007 ± 0.070	0.042 ± 0.035	0.052 ± 0.064	–0.003 ± 0.014
171990	0.034 ± 0.023	0.118 ± 0.070	0.068 ± 0.070	0.093 ± 0.049	0.038 ± 0.028	–0.017 ± 0.007
193193	0.002 ± 0.029	0.205 ± 0.070	–0.020 ± 0.064	0.055 ± 0.042	–0.010 ± 0.035	–0.005 ± 0.028
196800	–0.097 ± 0.060	0.063 ± 0.070	–0.007 ± 0.057	0.088 ± 0.035	–0.042 ± 0.064	–0.007 ± 0.070
199960	–0.021 ± 0.014	0.069 ± 0.070	–	0.059 ± 0.113	–0.056 ± 0.092	–0.021 ± 0.057
204385	0.005 ± 0.090	0.032 ± 0.070	–0.053 ± 0.035	0.052 ± 0.042	–0.003 ± 0.007	–0.018 ± 0.028
221356	–	0.115 ± 0.070	–0.175 ± 0.028	–0.070 ± 0.078	0.025 ± 0.071	–0.045 ± 0.028
31822	–0.061 ± 0.021	0.096 ± 0.070	–0.114 ± 0.070	–0.059 ± 0.049	–0.034 ± 0.070	–0.089 ± 0.035
36379	0.070 ± 0.026	0.110 ± 0.070	0.041 ± 0.070	0.055 ± 0.049	0.050 ± 0.042	–0.020 ± 0.014
3823	0.110 ± 0.085	0.227 ± 0.070	0.012 ± 0.064	0.032 ± 0.049	0.087 ± 0.071	–0.003 ± 0.042
38973	0.002 ± 0.025	–0.025 ± 0.070	–0.025 ± 0.057	0.025 ± 0.028	–0.030 ± 0.035	–0.030 ± 0.021
44120	–0.030 ± 0.038	–0.006 ± 0.070	–0.006 ± 0.070	0.069 ± 0.049	–0.036 ± 0.042	–0.016 ± 0.028
44447	0.060 ± 0.061	0.190 ± 0.070	–	0.030 ± 0.042	0.090 ± 0.085	–0.020 ± 0.014
6735	–0.029 ± 0.042	0.094 ± 0.070	–0.036 ± 0.127	–0.010 ± 0.035	–0.056 ± 0.042	–0.086 ± 0.028
68978A	–0.058 ± 0.017	–0.058 ± 0.070	–0.083 ± 0.134	0.002 ± 0.057	–0.003 ± 0.007	–0.048 ± 0.028
69655	0.026 ± 0.021	0.143 ± 0.070	–0.022 ± 0.021	0.053 ± 0.042	0.017 ± 0.021	–0.022 ± 0.021
70889	–0.127 ± 0.025	–0.044 ± 0.070	–0.079 ± 0.120	–0.044 ± 0.057	–0.064 ± 0.014	–0.104 ± 0.070
71479	–0.044 ± 0.035	0.133 ± 0.070	–0.057 ± 0.071	0.058 ± 0.106	–0.027 ± 0.057	–0.012 ± 0.007
73121	–0.053 ± 0.020	0.077 ± 0.070	–0.103 ± 0.070	0.037 ± 0.071	0.007 ± 0.070	0.007 ± 0.014
73524	–0.160 ± 0.007	–0.055 ± 0.070	–0.125 ± 0.071	–0.075 ± 0.042	–0.065 ± 0.085	–0.030 ± 0.035
88742	–0.003 ± 0.032	0.041 ± 0.070	–0.029 ± 0.071	–0.029 ± 0.057	–0.029 ± 0.014	–0.084 ± 0.021
95456	–0.068 ± 0.021	–0.012 ± 0.070	–0.012 ± 0.099	0.028 ± 0.057	–0.052 ± 0.014	–0.082 ± 0.028
9782	–0.002 ± 0.045	0.015 ± 0.070	–0.015 ± 0.099	0.025 ± 0.057	–0.055 ± 0.042	–0.060 ± 0.035
33636	–0.106 ± 0.015	0.061 ± 0.070	–0.114 ± 0.021	–0.039 ± 0.057	0.161 ± 0.070	–0.054 ± 0.021

Table A.6. Abundance ratios [X/Fe] of F-, G-type analogs without known planets

HD	[Si/Fe]	[Ca/Fe]	[Sc/Fe]	[Ti/Fe]	[V/Fe]	[Cr/Fe]
11226	0.012 ± 0.011	0.003 ± 0.017	0.032 ± 0.051	-0.021 ± 0.024	-0.030 ± 0.043	-0.007 ± 0.017
119638	0.027 ± 0.009	0.056 ± 0.028	0.023 ± 0.026	0.015 ± 0.023	-0.042 ± 0.026	-0.004 ± 0.022
122862	0.027 ± 0.009	0.041 ± 0.031	0.071 ± 0.026	0.015 ± 0.013	-0.035 ± 0.051	-0.003 ± 0.024
125881	-0.011 ± 0.022	0.023 ± 0.014	-0.019 ± 0.037	-0.019 ± 0.017	-0.043 ± 0.018	0.005 ± 0.010
1388	0.002 ± 0.014	0.036 ± 0.014	0.042 ± 0.043	0.007 ± 0.017	-0.072 ± 0.024	-0.007 ± 0.020
145666	-0.031 ± 0.010	0.019 ± 0.013	-0.052 ± 0.017	-0.014 ± 0.016	-0.077 ± 0.030	0.008 ± 0.012
157338	-0.002 ± 0.009	0.024 ± 0.023	0.009 ± 0.024	-0.008 ± 0.013	-0.056 ± 0.045	-0.006 ± 0.022
1581	0.030 ± 0.007	0.056 ± 0.018	0.040 ± 0.027	0.045 ± 0.027	-0.033 ± 0.055	-0.014 ± 0.020
168871	0.017 ± 0.017	0.056 ± 0.034	0.057 ± 0.043	0.007 ± 0.016	-0.030 ± 0.040	-0.007 ± 0.023
171990	0.022 ± 0.012	0.041 ± 0.047	0.060 ± 0.041	-0.005 ± 0.017	-0.028 ± 0.029	-0.012 ± 0.017
193193	0.010 ± 0.009	0.015 ± 0.018	0.063 ± 0.038	0.005 ± 0.016	-0.013 ± 0.025	-0.002 ± 0.019
196800	0.003 ± 0.017	-0.017 ± 0.014	0.045 ± 0.038	-0.025 ± 0.030	-0.002 ± 0.044	-0.010 ± 0.034
199960	0.015 ± 0.019	-0.021 ± 0.063	0.057 ± 0.035	-0.017 ± 0.035	0.007 ± 0.032	-0.008 ± 0.020
204385	0.011 ± 0.017	0.012 ± 0.022	0.042 ± 0.027	-0.013 ± 0.026	-0.058 ± 0.033	0.005 ± 0.018
221356	0.012 ± 0.012	0.069 ± 0.049	0.075 ± 0.016	0.088 ± 0.036	-0.069 ± 0.039	-0.025 ± 0.031
31822	-0.001 ± 0.014	0.054 ± 0.025	-0.022 ± 0.022	0.014 ± 0.040	-0.104 ± 0.028	0.005 ± 0.025
36379	0.044 ± 0.011	0.062 ± 0.029	0.070 ± 0.033	0.021 ± 0.024	-0.020 ± 0.053	0.006 ± 0.023
3823	0.061 ± 0.019	0.080 ± 0.021	0.072 ± 0.033	0.058 ± 0.029	-0.035 ± 0.050	-0.008 ± 0.020
38973	0.006 ± 0.012	0.021 ± 0.017	0.003 ± 0.030	-0.023 ± 0.019	-0.033 ± 0.035	0.004 ± 0.018
44120	0.004 ± 0.019	0.035 ± 0.049	0.031 ± 0.022	-0.020 ± 0.024	-0.008 ± 0.025	-0.020 ± 0.020
44447	0.039 ± 0.009	0.051 ± 0.016	0.058 ± 0.040	0.025 ± 0.019	-0.033 ± 0.055	-0.007 ± 0.020
6735	0.011 ± 0.012	0.057 ± 0.021	-0.002 ± 0.033	0.009 ± 0.034	-0.075 ± 0.047	-0.010 ± 0.019
68978A	0.001 ± 0.011	0.030 ± 0.023	-0.003 ± 0.017	-0.006 ± 0.013	-0.037 ± 0.039	0.011 ± 0.013
69655	0.019 ± 0.009	0.038 ± 0.024	0.025 ± 0.022	0.006 ± 0.019	-0.062 ± 0.043	-0.004 ± 0.013
70889	-0.028 ± 0.008	0.021 ± 0.024	-0.039 ± 0.045	-0.026 ± 0.027	-0.064 ± 0.023	0.008 ± 0.014
71479	-0.001 ± 0.019	-0.015 ± 0.026	0.083 ± 0.041	-0.003 ± 0.017	0.029 ± 0.022	-0.000 ± 0.019
73121	0.016 ± 0.015	0.015 ± 0.017	0.060 ± 0.036	-0.000 ± 0.024	-0.006 ± 0.043	-0.008 ± 0.026
73524	-0.008 ± 0.014	0.044 ± 0.030	0.005 ± 0.022	0.010 ± 0.020	-0.030 ± 0.024	0.006 ± 0.016
88742	-0.014 ± 0.013	0.019 ± 0.026	-0.044 ± 0.034	-0.029 ± 0.019	-0.043 ± 0.023	0.013 ± 0.016
95456	0.000 ± 0.014	0.028 ± 0.047	-0.009 ± 0.015	-0.010 ± 0.034	-0.060 ± 0.037	-0.003 ± 0.024
9782	-0.014 ± 0.020	-0.010 ± 0.048	-0.018 ± 0.021	-0.045 ± 0.018	-0.042 ± 0.044	-0.013 ± 0.019
33636	0.004 ± 0.006	0.051 ± 0.015	0.015 ± 0.042	0.041 ± 0.022	-0.031 ± 0.038	0.008 ± 0.027

Table A.7. Abundance ratios [X/Fe] of F-, G-type analogs without known planets

HD	[Mn/Fe]	[Co/Fe]	[Ni/Fe]	[Cu/Fe]	[Zn/Fe]	[Sr/Fe]
11226	-0.057 ± 0.058	-0.022 ± 0.016	0.004 ± 0.018	0.003 ± 0.070	0.008 ± 0.035	-0.036 ± 0.070
119638	-0.097 ± 0.036	-0.033 ± 0.025	-0.025 ± 0.014	0.006 ± 0.070	-0.014 ± 0.042	-0.035 ± 0.070
122862	-0.039 ± 0.070	-0.028 ± 0.010	-0.010 ± 0.013	0.044 ± 0.070	0.019 ± 0.007	-0.096 ± 0.070
125881	-0.057 ± 0.038	-0.069 ± 0.012	-0.024 ± 0.015	-0.027 ± 0.070	-0.017 ± 0.028	0.033 ± 0.070
1388	-0.082 ± 0.046	-0.038 ± 0.012	-0.021 ± 0.014	-0.008 ± 0.070	-0.043 ± 0.021	-0.008 ± 0.070
145666	-0.089 ± 0.045	-0.089 ± 0.007	-0.048 ± 0.015	-0.037 ± 0.070	-0.037 ± 0.042	0.053 ± 0.070
157338	-0.031 ± 0.071	-0.054 ± 0.024	-0.024 ± 0.012	-0.006 ± 0.070	0.019 ± 0.035	-0.026 ± 0.070
1581	-0.118 ± 0.039	-0.007 ± 0.022	-0.024 ± 0.014	-0.003 ± 0.070	0.007 ± 0.014	-0.043 ± 0.070
168871	-0.081 ± 0.106	-0.035 ± 0.016	-0.012 ± 0.013	0.027 ± 0.070	0.037 ± 0.028	-0.053 ± 0.070
171990	-0.056 ± 0.065	0.016 ± 0.028	0.013 ± 0.021	0.048 ± 0.070	0.033 ± 0.021	-0.062 ± 0.070
193193	-0.050 ± 0.026	-0.016 ± 0.021	-0.011 ± 0.015	0.005 ± 0.070	0.015 ± 0.014	-0.065 ± 0.070
196800	0.015 ± 0.015	0.015 ± 0.019	0.028 ± 0.017	0.013 ± 0.070	0.013 ± 0.057	-0.057 ± 0.070
199960	0.087 ± 0.025	0.059 ± 0.013	0.056 ± 0.028	0.059 ± 0.070	0.069 ± 0.113	-0.091 ± 0.070
204385	-0.024 ± 0.048	0.009 ± 0.014	0.001 ± 0.020	0.032 ± 0.070	0.036 ± 0.092	-0.128 ± 0.070
221356	-0.155 ± 0.073	-0.035 ± 0.035	-0.020 ± 0.037	0.075 ± 0.070	-0.105 ± 0.057	0.005 ± 0.070
31822	-0.162 ± 0.054	-0.086 ± 0.033	-0.057 ± 0.015	-0.004 ± 0.070	-0.099 ± 0.049	-0.004 ± 0.070
36379	-0.069 ± 0.078	-0.020 ± 0.023	-0.015 ± 0.015	0.030 ± 0.070	0.000 ± 0.070	-0.100 ± 0.070
3823	-0.153 ± 0.027	-0.002 ± 0.016	-0.013 ± 0.015	0.067 ± 0.070	-0.028 ± 0.078	-0.093 ± 0.070
38973	-0.045 ± 0.037	-0.031 ± 0.013	-0.001 ± 0.013	-0.005 ± 0.070	0.010 ± 0.035	-0.055 ± 0.070
44120	-0.016 ± 0.055	-0.016 ± 0.008	0.013 ± 0.015	0.014 ± 0.070	-0.001 ± 0.078	-0.076 ± 0.070
44447	-0.120 ± 0.039	-0.029 ± 0.033	-0.025 ± 0.015	0.020 ± 0.070	0.015 ± 0.021	-0.130 ± 0.070
6735	-0.144 ± 0.084	-0.061 ± 0.032	-0.042 ± 0.016	-0.025 ± 0.070	-0.050 ± 0.007	-0.005 ± 0.070
68978A	-0.082 ± 0.044	-0.028 ± 0.019	-0.017 ± 0.014	-0.028 ± 0.070	-0.143 ± 0.007	-0.218 ± 0.070
69655	-0.095 ± 0.039	-0.011 ± 0.015	-0.016 ± 0.018	0.013 ± 0.070	0.032 ± 0.085	-0.057 ± 0.070
70889	-0.024 ± 0.024	-0.082 ± 0.016	-0.033 ± 0.009	-0.064 ± 0.070	-0.074 ± 0.028	0.046 ± 0.070
71479	0.037 ± 0.043	0.033 ± 0.018	0.041 ± 0.015	0.023 ± 0.070	0.003 ± 0.042	-0.037 ± 0.070
73121	-0.033 ± 0.033	-0.021 ± 0.013	0.001 ± 0.017	0.007 ± 0.070	0.002 ± 0.035	-0.033 ± 0.070
73524	-0.060 ± 0.024	-0.022 ± 0.013	-0.012 ± 0.015	-0.045 ± 0.070	-0.095 ± 0.042	0.055 ± 0.070
88742	-0.057 ± 0.022	-0.071 ± 0.022	-0.034 ± 0.014	-0.069 ± 0.070	-0.044 ± 0.007	0.031 ± 0.070
95456	-0.029 ± 0.039	-0.035 ± 0.022	-0.010 ± 0.018	-0.002 ± 0.070	-0.047 ± 0.007	-0.012 ± 0.070
9782	-0.020 ± 0.029	-0.038 ± 0.020	-0.005 ± 0.019	-0.025 ± 0.070	-0.050 ± 0.035	-0.025 ± 0.070
33636	–	-0.062 ± 0.016	-0.047 ± 0.017	-0.079 ± 0.070	-0.039 ± 0.070	–

Table A.8. Abundance ratios [X/Fe] of F-, G-type analogs without known planets

HD	[Y/Fe]	[Zr/Fe]	[Ba/Fe]	[Ce/Fe]	[Nd/Fe]	[Eu/Fe]
11226	0.030 ± 0.029	0.044 ± 0.070	0.048 ± 0.106	-0.047 ± 0.030	-0.117 ± 0.070	0.003 ± 0.070
119638	0.056 ± 0.035	0.096 ± 0.070	0.126 ± 0.042	-0.001 ± 0.076	-0.054 ± 0.070	0.046 ± 0.070
122862	0.000 ± 0.046	0.034 ± 0.070	0.024 ± 0.028	-0.046 ± 0.060	-0.056 ± 0.070	0.074 ± 0.070
125881	0.103 ± 0.010	0.133 ± 0.070	0.148 ± 0.049	0.019 ± 0.038	-0.027 ± 0.070	0.063 ± 0.070
1388	0.048 ± 0.021	0.072 ± 0.070	0.067 ± 0.007	0.028 ± 0.025	-0.078 ± 0.070	0.042 ± 0.070
145666	0.119 ± 0.012	0.133 ± 0.070	0.198 ± 0.007	0.096 ± 0.029	0.003 ± 0.070	0.033 ± 0.070
157338	0.057 ± 0.015	0.074 ± 0.070	0.129 ± 0.106	-0.003 ± 0.025	-0.086 ± 0.070	0.014 ± 0.070
1581	0.040 ± 0.023	0.107 ± 0.070	0.097 ± 0.028	0.040 ± 0.050	0.007 ± 0.070	0.097 ± 0.070
168871	0.024 ± 0.029	0.057 ± 0.070	0.052 ± 0.021	-0.006 ± 0.021	-0.083 ± 0.070	0.077 ± 0.070
171990	0.044 ± 0.038	0.048 ± 0.070	0.043 ± 0.021	-0.032 ± 0.061	-0.102 ± 0.070	0.028 ± 0.070
193193	0.015 ± 0.026	-0.015 ± 0.070	0.060 ± 0.021	-0.018 ± 0.029	-0.095 ± 0.070	-0.015 ± 0.070
196800	0.013 ± 0.026	-0.067 ± 0.070	-0.037 ± 0.014	-0.034 ± 0.092	-0.127 ± 0.070	-0.167 ± 0.070
199960	-0.008 ± 0.075	0.009 ± 0.070	-0.076 ± 0.035	-	-0.161 ± 0.070	0.059 ± 0.070
204385	0.045 ± 0.023	-0.048 ± 0.070	0.061 ± 0.028	-0.035 ± 0.050	-0.088 ± 0.070	-0.008 ± 0.070
221356	0.052 ± 0.061	0.075 ± 0.070	0.215 ± 0.014	-	0.065 ± 0.070	0.145 ± 0.070
31822	0.092 ± 0.012	0.096 ± 0.070	0.271 ± 0.035	0.122 ± 0.086	0.066 ± 0.070	-0.094 ± 0.070
36379	-0.020 ± 0.044	0.020 ± 0.070	0.030 ± 0.042	-0.050 ± 0.026	-0.089 ± 0.070	0.041 ± 0.070
3823	-0.043 ± 0.053	0.017 ± 0.070	-0.028 ± 0.021	-0.033 ± 0.050	-0.083 ± 0.070	0.077 ± 0.070
38973	0.052 ± 0.021	0.035 ± 0.070	0.030 ± 0.035	-0.042 ± 0.035	-0.075 ± 0.070	0.025 ± 0.070
44120	0.014 ± 0.026	0.014 ± 0.070	0.019 ± 0.007	-0.046 ± 0.020	-0.116 ± 0.070	0.034 ± 0.070
44447	-0.047 ± 0.049	-0.010 ± 0.070	-0.010 ± 0.014	-0.050 ± 0.062	-0.100 ± 0.070	0.030 ± 0.070
6735	0.101 ± 0.029	0.134 ± 0.070	0.194 ± 0.028	0.041 ± 0.137	-0.036 ± 0.070	-0.005 ± 0.070
68978A	0.079 ± 0.029	0.042 ± 0.070	0.122 ± 0.028	0.032 ± 0.017	-0.068 ± 0.070	-0.098 ± 0.070
69655	0.002 ± 0.026	0.023 ± 0.070	0.058 ± 0.007	-0.007 ± 0.017	-0.047 ± 0.070	0.032 ± 0.070
70889	0.113 ± 0.012	0.116 ± 0.070	0.176 ± 0.028	0.053 ± 0.015	-0.084 ± 0.070	-0.054 ± 0.070
71479	0.010 ± 0.051	-0.017 ± 0.070	-0.047 ± 0.028	-0.044 ± 0.049	-0.157 ± 0.070	-0.027 ± 0.070
73121	0.067 ± 0.044	0.047 ± 0.070	0.107 ± 0.042	0.020 ± 0.046	-0.083 ± 0.070	0.067 ± 0.070
73524	0.085 ± 0.040	0.105 ± 0.070	0.095 ± 0.014	0.042 ± 0.025	-0.055 ± 0.070	0.045 ± 0.070
88742	0.097 ± 0.021	0.131 ± 0.070	0.151 ± 0.014	0.051 ± 0.030	-0.049 ± 0.070	-0.039 ± 0.070
95456	0.078 ± 0.044	0.058 ± 0.070	0.028 ± 0.070	-0.025 ± 0.032	-0.052 ± 0.070	-0.052 ± 0.070
9782	0.058 ± 0.015	0.045 ± 0.070	0.030 ± 0.021	-0.065 ± 0.078	-0.145 ± 0.070	-0.045 ± 0.070
33636	0.101 ± 0.017	0.141 ± 0.070	0.191 ± 0.014	-	0.071 ± 0.070	0.051 ± 0.070